Stockholm University

Master Thesis

Degree Project in Geochemistry 45 hp

Methane oxidation on the East Siberian Shelf – An incubation experiment

Tomas Schedwin

Stockholm 2016

Department of Geological Sciences
Stockholm University
SE-106 91 Stockholm
Sweden

1 Introduction 5
1.1 Methane cycle 6
1.2 Microbial methane formation 6
1.3 Microbial methane oxidation 7
1.4 Methane isotope studies 8
1.5 Aim of the study 10
2 Materials and method 12
2.1 Incubation 12
2.2 Analytical method 14
3 Method development 20
3.1 Injection method 20
3.2 Stabilization time 23
3.3 Reproducibility and long term stability 24
3.4 Accuracy 26
3.5 Concentration dependence of the isotope signal 26
3.6 Possible interference effects 27
3.7 CH_4 concentration measurement – Picarro 28
3.8 Conclusion 29
4 Pilot experiment – Brunnsviken 31
4.1 Experimental set up 32
4.2 Starting conditions 33
4.3 Experimental results – GC-IRMS vs Picarro 35
4.4 Experimental results – incubation time series 36
4.5 Discussion Brunnsviken 38
4.6 Conclusion pilot experiment 41
5 Main experiment - East Siberian shelf 42
5.1 Experimental set up 43
5.2 Experimental results 44
5.3 Discussion 47
6 Conclusion and outlook 49
6.1 Possible improvements 50

7 Acknowledgements 51
8 References 53
9 Appendix 60

Cover photo by Julia Steinbach

Abstract

Methane is one of the most significant greenhouse gases and has a radiative forcing 23 times higher than carbon dioxide and methane in the atmosphere has increased with a 2.5times since the industrial era. The East Siberian Shelf is a crucial area to study the carbon and methane cycle since it is believed to hold large amounts of carbon in the subsea permafrost that could potentially be released into the water column. Increased knowledge of the sources and sinks in this area is crucial to estimate future emissions. In this thesis the oxidation in the water column and sediments in the East Siberian Shelf were investigated using an incubation method. The best method for analyzes of the isotopic carbon composition was determined in a number of initial tests where the performance of a cavity ring-down system from Picarro compared to a gas chromatograph isotope ratio mass spectrometer (GC-IRMS). The results showed that the Picarro performed well with a reproducibility of ±0.56‰ a difference of 3.44±1.03‰ and 2.08±1.09‰ compared to the GC-IRMS. The incubation method was tested using samples from the small estuary of Brunnsviken in Stockholm. The oxidation rate in the samples ranged from approximately 100 to 8000nM/day depending on the depth. The isotopic fractionation was calculated from 27.6 to 14‰. In the main experiment of using water and sediment form the East Siberian Shelf a matrix of sub experiments was set up with samples containing only water and samples containing sediment and water. The different sub experiments contained a different amount of CH_4 and were incubated in different temperatures. The results showed that there is no CH_4 oxidation in the water column and no oxidation in the samples containing sediment and water incubated at 20°C. Oxidation occurred only in the samples that contain sediment and water that was incubated at 4°C indicating a psychrophilic bacterial community. The oxidation rate was calculated to be 19nM/day and the isotopic fractionation was 15.3‰.

1 Introduction

Methane (CH_4) is one of the most abundant hydrocarbons in the atmosphere and is one of the most significant greenhouse gases. It is believed to have a great effect on climate since the radiative forcing is up to 23 times higher than carbon dioxide (Grant & Whiticar, 2002). Both paleorecord and modern studies suggest that methane emissions have a great feedback on the climate. Since the pre-industrial era methane in the atmosphere has increased by a factor of 2.5 (Dlugokencky et al, 2011), a value that is predicted to double by the year 2100 (Myhre et al., 2013).

Marine environments have not been considered as a significant source of methane for the atmospheric budget (e.g. Reeburgh, 2007; Dlugokencky et al, 2011). Methane is transported from sediments by ebullition or diffusive transport, however the methane is thought to oxidize to a large extent in the sediment and the water column and therefore is thought to only contribute with approximately 2% to the global methane budget (Reeburgh, 2007).

Elevated methane concentrations in the water column have been found in the East Siberian Shelf (e.g. Shakhova et al., 2010b; Shakhova et al., 2005). The source of the methane is under discussion, however, it indicates that there is methane mobilization (Ciais et al, 2013). It is believed that the continental shelf of the East Siberian shelf and slope hold large amounts of carbon in the form of methane hydrates, subsea permafrost and free gas trapped below permafrost. Shakhova et al., 2010b estimated that the permafrost holds up to 1400Gt of organic carbon and 360 Gt of methane trapped as free gas trapped below the permafrost. The size of the methane hydrate reservoir has been estimated to contain an additional 540Gt of methane. Global warming will most likely impact the arctic more than other latitudes (Collins et al., 2013; Mann et al., 1999) with a predicted temperature rise of 2-9°C by year 2100 (Anisimov et al., 2007) that could potentially destabilize the reservoirs and have a positive feedback on the climate.

The release of the potential methane reservoirs may happen in two scenarios; a smooth release due to methane diffusion from reservoirs in the bottom and a sharp release due

to destruction of methane hydrates and ebullition (Shakhova et al 2010a). Therefore understanding the sources of the methane is critical to estimate future emissions.

To gain further knowledge of the processes that are active in the East Siberian Sea, isotopic tracing of the sources of methane is a useful tool; different sources have different methane isotopic composition (figure 1.2). Since microbial oxidation alters the isotopic composition of CH_4, source tracing becomes more complicated. Quantifying the degree to which isotopic fractionation during microbial oxidation varies in different environments is critical to gain further understanding on the sources of the emissions.

In this study the oxidation rate and the carbon isotopic fractionation of aerobic methane oxidation in the East Siberian Shelf was investigated.

1.1 The biogenic methane cycle

1.1.1 Microbial methane formation

Microbial methane is the product of microbial breakdown of organic matter in anoxic sediment formed by the arachaeal group, the methanogens (figure 1.1). Methanogens is a part of the degradation of larger organic molecules (Wolin et al, 1987; Whiticar et al, 1986; Whiticar, 1999; Coleman et al, 1981) to produce methane. The methane in a marine setting is produced in buried sediments below the sulfate reduction zone, where the sulfate is depleted, in environments where the loading of organic material is high such as continental shelf (Deborde et al. 2009; Ferry et al., 2008)(figure 1.4). Formation of methane does not yield much energy and is formed when other electron acceptors (O_2, NO_3^-, Mn(IV), Fe(III), SO_4^{2-}) in the sediment are depleted (Jørgensen and Kasten, 2006). Therefore roughly 2-5% of the remineralization of organic matter is due to methanogenesis in marine sediments (Deborde et al., 2010). Methane on continental shelves can also be derived from flooded terrestrial permafrost (Shakhova et al., 2010).

There are a variety of substrates that can be used by the methanogens to form methane for example CO_2-H_2, acetate, formate and methanol where CO_2-H_2 (carbonate reduction) and acetate fermentation are the most globally significant pathways of methanogenesis (Wolin et al. 1987; Conrad, 2005).

The reaction pathway of acetate fermentation can be expressed in equation 1:

$$CH_3COOH \rightarrow CH_4 + CO_2$$

While carbonate reduction is expressed by the reaction in equation 2:

$$CO_2 + 4H_2 \rightarrow CH_4 + 2H_2O$$

Both of these pathways are considered competitive pathways meaning that the substrate is sought after and more efficiently utilized by other microbial consortia such as sulfur reducing bacteria (Whiticar, 1999).

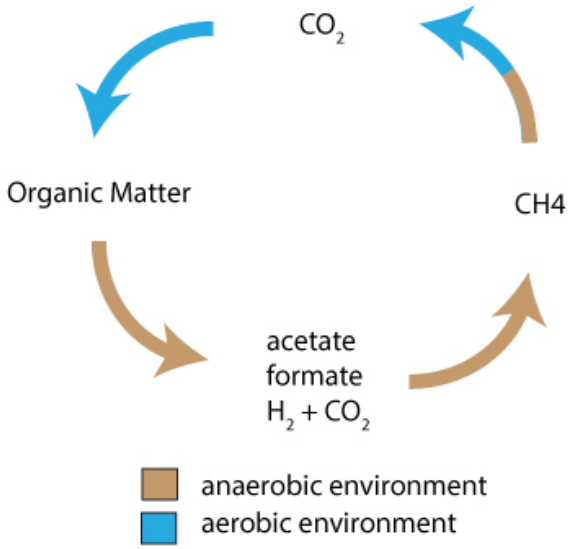

Figure 1.1 – the methane cycle from fixation of carbon dioxide in organic matter to oxidation back to carbon dioxide. Modified version from Ferry et al., 2008

1.1.2 Microbial methane oxidation

Microbial oxidation is an important sink for methane and without it the atmospheric concentration of methane could be several magnitudes greater. Since methane is not reactive in aquatic systems at ambient temperature it requires microbial activity to be able to oxidize back to CO_2 (Jørgensen and Kasten, 2006). In a marine environment microbial oxidation of methane occurs in the sediment and the water column under both aerobic conditions and anaerobic conditions (Deborde et al. 2009). The reaction that oxidizes CH_4 to CO_2 is expressed as:

$$CH_4 + 2O_2 \rightarrow CO_2 + 2H_2O$$

CH_4 oxidation in anaerobic marine sediments occurs underneath the sulfate reduction zone. The evidence for this process is decrease in CH_4 concentration within the sulfate methane transition zone compared to other hydro carbonates and a shift in the isotopic composition of the methane throughout the zone (Whiticar, 1999; Jørgensen and Kasten, 2006). Not all the CH_4 is however oxidized in the sediments and small amount are able to persist in the sulfate reduction zone (Whiticar and Faber, 1986).
Aerobic methanotrophs uses oxygen to oxidize methane by the enzyme methane monooxygenase. Aerobic oxidation gives a higher energy yield compared to anaerobic oxidation (Jacobs et al., 2013). The CH_4 released from the ocean is related to the rate of CH_4 production and oxidation in the sediments and water column (Deborde et al. 2009).

1.2 Methane isotope studies

The isotopic composition of carbon and hydrogen can be used to trace the sources and sinks of methane when physical processes and chemical reactions discriminate against either heavy or light isotopes. The final isotopic signature depends on two factors, (1) the isotopic composition of the source material and (2) the kinetic isotope effect (KIE). The KIE means that the material with a lower isotopic mass will react and diffuse more rapidly than the molecule with a higher isotopic mass. This is particularly true in biotic processes that strongly discriminate against heavier isotopes containing stronger chemical bonds and lower diffusivity. This ultimately creates a lighter product in a metabolic reaction.

Carbon has two stable isotopes, ^{12}C and ^{13}C where 98.89% consists of the lighter isotope. The isotopic composition of the methane is given in the commonly used δ notation (Coplen, 2011) where the δ is expressed in permil (‰) by equation 3:

$$\delta = \left[\frac{(R_a)Sample}{(R_a)Standard} - 1\right] * 10^3$$

Equation 3

Where R_a(Sample) and R_a(Standard) are the $^{13}C/^{12}C$ ratio of the sample and a standard, the international standard for $\delta^{13}C$ is the Vienna Pee Dee Belemnite (VPDB).

Isotopic fractionation gives a different isotope signature for substrate and product. The fractionation can be expressed by a fractionation factor (α) (Coplen, 2011) and the isotopic separation can be described by the isotopic fractionation (ε).

1.2.1 Carbon isotope signature of microbial methane

Methane production by microbial consortia shows a wide range of $\delta^{13}C\text{-}CH_4$ compositions (figure 1.2) but is generally depleted in $\delta^{13}C\text{-}CH_4$ (-100‰ to -50‰) compared to methane formed by thermogenic processes (-50‰ to -20‰) (eg Whiticar, 1999; Coleman et al., 1981). The two common microbial pathways, carbonate reduction and acetate fermentation both fractionate carbon isotopes compared to the source material (organic matter or CO_2). Methane from acetate fermentation is relatively enriched in ^{13}C and methane produced by carbonate reduction is more depleted in ^{13}C. The difference in $\delta^{13}C\text{-}CH_4$ between the pathways is around -60‰. The two depositional environments can be tracked by the in $\delta^{13}C\text{-}CH_4$ since carbonate reduction is associated with saline/marine environment and acetate fermentation is associated with a freshwater environment (Whiticar et al., 1986; Whiticar, 1999) (figure 1.2).

Figure 1.2 - the boundaries of the d13C signal with respect to formation environment based on information from Whiticar 1999.

As methane is oxidized to CO_2 by methanotrophic bacteria (MOB) the isotopic composition of carbon is altered as the lighter carbon isotope reacts more rapidly than the heavy via the kinetic isotope effect (described above). This leaves the residual methane more enriched in ^{13}C and can thus show a signature that can be confused with other sources (e.g. thermogenic). The discrimination against the heavier isotopes is considered small as long as the concentration of methane remains high (above 1μM). Significant shift in the $\delta 13C\text{-}CH_4$ becomes more apparent as the concentration becomes low (0.4 μM) (Whiticar, 1986).

Isotopic fractionation associated with aerobic methane oxidation has been investigated in a number of studies both in the field (e.g. Gamo et al (2009)) and in laboratory (e.g. Coleman et al., (1981) and Feisthauer et al., (2011)). Coleman et al. (1981) used cultures from two different sources that was incubated in different temperatures over a period of time and monitored for signs of methane oxidation. Feisthauer et al. (2011) used different strains of methanotrophs under different copper concentrations to determine the isotopic fractionation during the experiment. The factors that have been discovered show a large spread varying from a 3‰ up to 39‰ for laboratory studies (table 1.1). Field studies generally show a lower isotopic fractionation than laboratory studies. In the field non-oxidized methane may enter the system and lower the fractionation while in a laboratory study usually no new methane is added. This would increase the isotopic fractionation in laboratory experiments.

Laboratory incubation		
Source	**Process**	**$\varepsilon_{methane}$**
Coleman et al. (1981)	Aerobic oxidation	13 to 25
Templeton et al. (2006)	Aerobic oxidation	3 to 39
Holler et al. (2009)	Anaerobic oxidation	12 to 39
Feisthauer et al. (2011)	Aerobic oxidation	14.8 to 27.8
Field Studies		
Source	**Area**	**$\varepsilon_{methane}$**
Grant and Whiticar (2002)	Marine cold seep, Hydrate Ridge	2 to 13
Gamo et al. (2010)	Hydrothermal plume, Okinawa Trough	12
Damm et al. (2007)	Arctic marine water	17

Table 1.1 isotopic fractionation collected from previous aerobic methane oxidation studies conducted in a laboratory environment.

1.3 Aim of the study

Since the marine arctic permafrost may contain large quantities of carbon and since the artic is projected to be warming between 2 and 9°C during a global climate change it is important to understand the removal pathways and sources of greenhouse gases in the region. Understanding the oxidation in water and sediments will help understand the sources of methane in the water column and atmosphere of the East Siberian Shelf and the importance of methane oxidation in the removal of methane.

The goal of this thesis was to study the methane oxidation in the water column and in sediment of the East Siberian shelf and to determine the strength of the isotopic fractionation. To do this:

An analytical method was developed to prepare and analyze samples and to measure the isotopic composition of discrete water sampled on a Picarro cavity ring-down laser spectrometer.

A set of incubation experiments was conducted with water and sediment samples collected in the summer of 2014 during the SWERUS expedition on icebreaker Oden to the Eastern Siberian Shelf Sea.

The dependence of isotopic fractionation on different environmental parameters was tested.

With these experiments the central hypothesis to be addressed was whether:

1. Significant oxidation of methane occurs in the water column and the sediment of the East Siberian Shelf.

2. Methane oxidation is associated with strong isotopic fractionation.

3. The isotopic fractionation factor is controlled by the methane oxidation rate.

4. The methane oxidation rate is dependent on the water temperature and presence of sediment bacteria.

2 Materials and method

2.1 Incubation

Incubation is a commonly used method to study methane oxidation (e.g. Coleman et al., 1981; Templeton et al, 2005; Kinnaman et al., 2006). Incubation means that a water or sediment sample is monitored in a controlled environment that is favorable for methane oxidizing (methanotrophics) organisms. The samples are monitored for signs of methane oxidation e.g. changes in isotopic composition and decreases in concentration. These changes depend on a number of parameters such as environmental conditions (temperature and concentration) and methanotrophic community. A change in environmental conditions can help to increase the speed of the oxidation. Incubation of water/sediment samples can be performed with a headspace or without a headspace. The advantage of incubating with a headspace is that multiple gas samples can be extracted from a single sample while in a headspace free incubation only one time point per sample can be analyzed.

In this study headspace free incubation was used due to the simplicity of the method but also in an attempt to recreate a natural environment where all the methane is dissolved in the water. Also the volume of headspace needed for the analysis in this study would also change the concentration greatly in the sample since the Picarro analyzer needs around 20ml.

2.1.1 Kinetic isotope effect

Methane oxidation creates a shift in the isotopes composition of the residual methane towards more enriched in $\delta^{13}C$ (heavier). The isotopic composition as well as methane concentration will be monitored. As determined by previous studies the fractionation is dependent on a number of factors such as temperature and concentration (e.g. Coleman et al., 1981).

Since the incubation is performed with a closed system where no methane is added/removed a Rayleigh approach can be used to determine isotopic fractionation factor (ε) of the oxidation.

The calculation of the Rayleigh curve is based on the Rayleigh distillation equation (Scott et al, 2003)

$$\left(\frac{R}{R_0}\right) = (\frac{C}{C_0})^{\frac{1}{\alpha}-1}$$

Equation 4

Where R is the isotope ratio, C is the methane concentration and α is the fractionation factor. Instead of α, often the factor ε is used that is related to α by equation 5

$$\alpha = \frac{1}{\varepsilon + 1} * 1000$$

Equation 5

where ε is represented in ‰.

The original Rayleigh equation can be used to get a linear fit of the measured values with equation 6

$$\ln\left(\frac{R}{R_0}\right) = \varepsilon * ln\left(\frac{C}{C_0}\right)$$

Equation 6

The expression $\ln(R/R_0)$ can be re-written to be able to use the isotopic composition values measured during the study with 7equation 7

$$ln\frac{R_{sample}}{R_{standard}} = \ln\left(\frac{\delta^{13}C_{CH4}}{1000} + 1\right)$$

Equation 7

This way, a plot with using $\ln(C/C_0)$ on the x-axis and ln(d13C-CH4/1000+1) on the y-axis can be created, where the slope of the regression line represents the isotopic fractionation (ε).

Once ε is calculated a non-logarithmic model based on the isotopic fractionation is created can be to estimate where in the oxidation sequence a sample is. The equation for the residual methane model is:

$$\delta_{Residual} = \delta_{start} + (\varepsilon * lnf)$$

Equation 8

where δ_{start} is the start isotopic composition, ε is the fractionation factor and $lnf=ln(C/C_0)$ is the logarithm of the residual methane factor.

2.2 Analytical method

2.2.1 Head space technique

For measuring the concentration and isotopic composition of dissolved methane in the samples a headspace is used needed to extract the methane from the water. When a (methane free) gas such as nitrogen or helium is added to (or on top of) the sample the dissolved methane in the water strives to reach equilibrium with the overlaying headspace. Between 80 and 90% of the dissolved methane is transferred to the headspace. This results in a transfer of the methane from the water to the headspace.

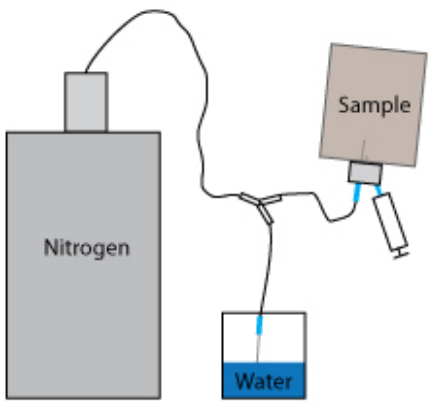

Figure 2.1 - The procedure to set headspace on the samples using a three way valve to ensure 1atm in the heaspace.

In this work nitrogen (N_2, purity 99,999%) is used as headspace. Prior and after the addition of headspace the sample flasks are weighed in order to calculate the exact amount of headspace introduced. To ensure that the pressure in the headspace is approximately 1 atm a three-way valve is used (figure 2.1).

The samples are shaken on a shaker table for one hour to let the methane in the sample equilibrate with the headspace.

To calculate the concentration of CH_4 the formula given in Bange et al. (2010) was used

$$[CH_4]=x'PV_{hs}/(RTV_{wp})+x'\beta P$$

Equation 9

Where x' is the dry mole fraction in the headspace, P is the pressure, V_{hs} and V_{wp} the volume of head space and water phase, R is the gas constant, T is the temperature of the equilibrium, β is the Bunsen solubility coefficient.

The Bunsen solubility coefficient of methane (β) is taken from the equation given in Wisenburg and Guinasso (1979). The Bunsen coefficient enables calculations of gases in sea and freshwater that is in equilibrium with the atmosphere. The Bunsen coefficient is calculated using equation 10:

$$\ln \beta = A1 + A2 \left(\frac{100}{T}\right) + A3 \ln\left(\frac{T}{100}\right) + A4 \left(\frac{T}{100}\right)\text{^}2 + S \left[B1 + B2\left(\frac{T}{100}\right) + B3\left(\frac{T}{100}\right)^2\right]$$

Equation 10

where A1, A2, A3, A4, B1, B2, B3 are constants from Wisenburg and Guinasso (1979), T is the temperature of the head space in kelvin and S is the salinity in ppt.

2.2.2 Methane concentration analysis

Methane concentration in the headspace was measured using a gas chromatograph with a flame ionization detector and methanizer (GC-FID, SRI 8610C) available at Stockholm University. The instrument uses a stainless steel column packed with HayDep D and a 1ml injection loop. Nitrogen (N_2) is used as a carrier gas at a pressure of 4bars and 20ml/min flow rate. The oven temperature is 60°C and the methanizer and detection temperatures are 330°C. For each day and session of measurements a calibration curve is created using standards of 1.9ppm (air), 5ppm, 100ppm, 1000ppm and 10 000ppm of methane. To get a good statistical representation every standard was measured 3 times. The sample/standard volume that was injected into the gas chromatograph was 5ml. The areas of the methane peaks produced by the gas chromatograph were converted to ppm using the regression line given by the standard measurements.

2.2.3 Isotope analysis

The $\delta^{13}C$-CH_4 composition of the samples was measured using two techniques: A Cavity ring down spectroscopy analyzer from Picarro (G2201-i) and the standard method for

measuring carbon and hydrogen isotopes at Stockholm University, gas chromatograph isotope ratio mass spectrometer (GC-IRMS).

2.2.3.1 GC-IRMS

The GC-IRMS used at Stockholm University is a Delta V Plus isotope mass spectrometer that is connected to a GC/C-GC/TC from ThermoScientific. The methane in the sample is separated from other gases using a CP-PoraPLOT Q GC column and oxidized to carbon dioxide by reacting with nickel oxide at a temperature of 1000°C. After the oxidation the gas is transferred to the IRMS and the isotopic composition can be calculated using the ^{12}C and $1^{3}C$ peaks of the sample. Samples that contain concentration 0.5% CH_4 or more can be injected directly into the system using a syringe. For samples with a lower concentration (as expected in this study) the methane needs to be pre-concentrated before analyze using a "Precon system" (Rice et al 2001). Here the sample is injected into a sample loop (10ml for samples with a concentration of 2-20ppm CH_4, 2ml for concentration between 20 and 300ppm). A cryotrap removed CO2 and water from the sample to minimize interference with the methane signal. Methane is then trapped in a steel trap packed with HayeSep molecular absorbance at a temperature of -120°C (consists out of a liquid nitrogen- ethanol slurry). After a pre-concentration time of 10min, the trap is warmed to release the methane into a third trap cryotrap (a GC column emerged in liquid nitrogen) to cryo-focus and from that trap the methane is led into the GC-IRMS system. The analytical precision of this system is 0.1‰ for direct injections and 0.3‰ for the samples that have been pre-concentrated.

Analysis time for a single analysis is approximately 10min if using the direct injection, and approximately 30min if using the pre-con system. The system needs daily calibration and control of the system using a 100% CH_4 calibration standard and a 5ppm control standard. This takes around 3.5 hours.

This makes it worth investigating if a less time-consuming system such as the Picarro can preform comparably to the GC-IRMS.

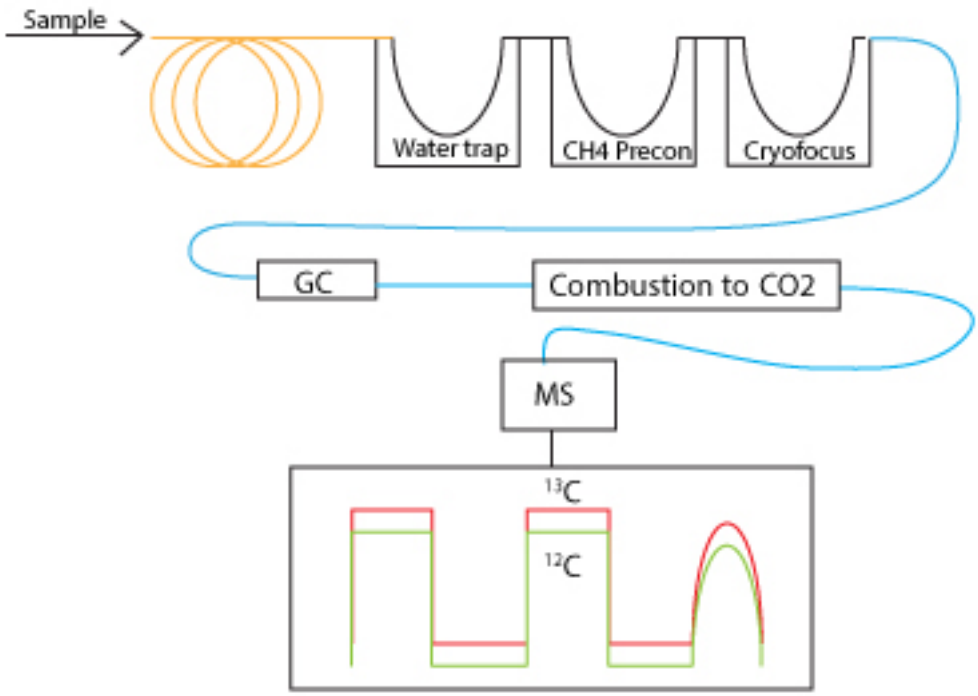

Figure 2.2 – A schematic overview of a measurement conducted with the GC-IRMS

2.2.3.2 Picarro - Cavity ring down spectroscopy

The Picarro analyzer is a cavity ring-down analyzer (CRDS) (figure 2.5a) that works with the absorption spectrum of small molecules that are in gas phase. The CRDS consists of a single frequency laser that is introduced into a cavity. The cavity consists out of three mirrors that elongate the lasers path length greatly and a photo detector that record small changes in the light intensity. A CRDS works in two phases, a Build-Up phase and a Ring-Down phase. In the Build-Up phase the laser beam is introduced into the cavity and is reflected by the mirrors. In the Ring-Down phase the laser is turned off and the photo detector measures the decay of the light from the laser through scattering and absorption of the sample. The Ring-Down time is directly proportional to the amount of sample in the cavity and the Picarro calculates the concentration of the sample by relating the Ring-Down time with a sample

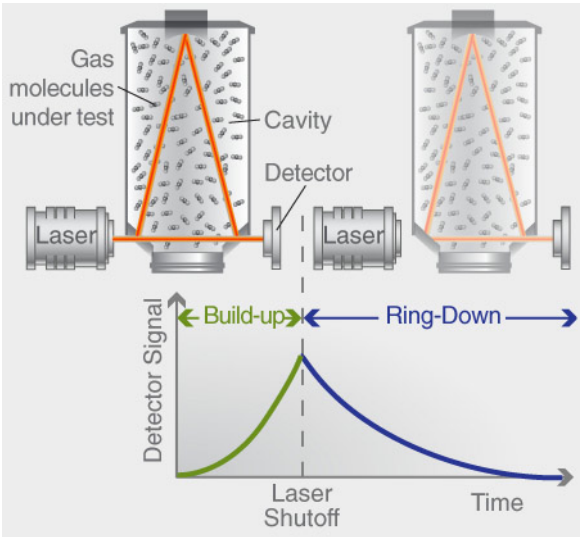

Figure 2.3 - a overview of a measurement with a CRDS Source: www.picarro.com

introduced by a Ring-Down time with an empty cavity (figure 2.3) (Crossin, 2008; Roberts and Alan, 2015, Cavity Ring-Down Spectroscopy (CRDS) | Picarro, 2016). Figure 4 shows a scheme on a measurement using a CRDS.

The Small Sample Isotope Module (SSiM) (figure 2.4 and 2.5d) is a module that enables the Picarro G2201-I analyzer to measure discrete samples (down to 20ml). The SSiM consists of a sample chamber that is evacuated by an external vacuum pump (figure 2.5b). The sample is expanded in the chamber and analyzed with the Picarro G2201-I.

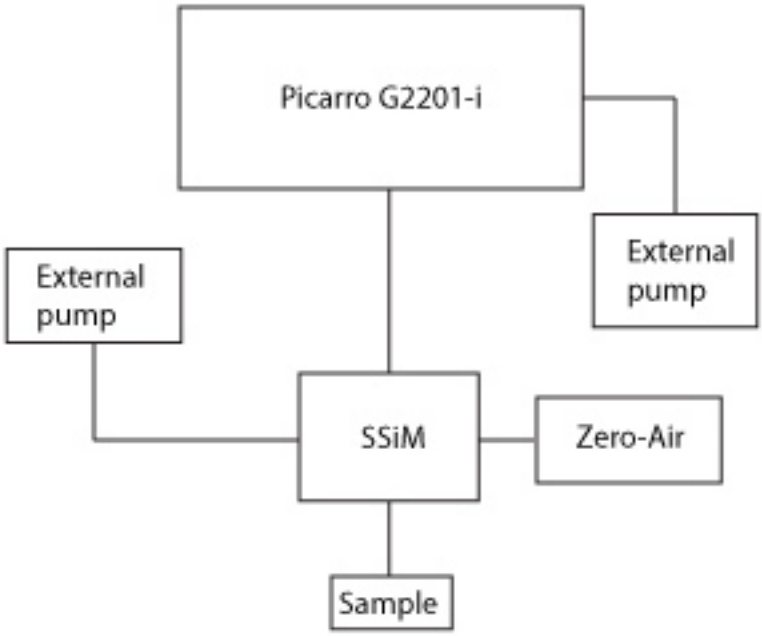

Figure 2.4 - A schematic overview of the Picarro set up

Since the Picarro G2201-i analyzer is optimized for precise measurements between 1.8 ppm up to 12ppm it is recommended to dilute samples with high concentration. That can either be done automatically by the SSiM or manually. The analytical precision of the sample at a concentration of 1.8ppm is <1,6‰ and at 10ppm the analytical precision is 0,8‰ (Picarro Small Sample Isotope Module (Model #A0314 User's Manual).
The Picarro measures the concentration of CO_2 and CH_4 as well as the $\delta^{13}C$ of these species. It does not need frequent calibration (currently running on the factory calibration made in 2013) but calibration of the analyzer using standard gases could improve the performance of the analyzer. The total time for one measurement is around

10 minutes where 7 minutes is the measurement time and 3 minutes are needed for evacuating the SSiM and injecting the sample.

Figure 2.5 - The Picarro set up in the lab with a) the Picarro analyzer, b) external pump for the SSiM, c) external pump for the Picarro analyzer, d) the SSiM with a tedlar bag connected.

3 Method development

Before starting the main experiment on samples from the East Siberian shelf, both the measurement technique (this chapter) and the incubation method (pilot experiment, described in chapter 4) were tested. A number of tests were set up to quantify the performance of the Picarro and to determine what is the best way to measure discrete samples with it. The long-term stability of the instrument, reproducibility/precision and accuracy of the measurements were tested using a 5ppm CH_4 standard (Picarro working standard) and compared to the GC-IRMS. The isotopic composition of the Picarro working standard had not been determined prior to this study and had been used as a concentration standard.

3.1 Injection method

To inject the sample, the SSiM is equipped with a 1/8 Swagelok tube fitting. This enables the operator to connect various types of sample containers like vial, syringes, tedlar bag or cylinders. The injection into the sample chamber works in two stages. In the first stage the syringe or sample bag is connected to the SSiM with its valves closed and the SSiM is evacuated. In the second stage the operator is asked to open the valves to the bag or syringe. The sample is at this stage sucked into the analyzer by the vacuum in the SSiM. Here two methods were tested; Injection was made with a syringe (picture 3.1 a) through a septum and using a tedlar bag (picture 3.1b) that had been modified with a Swagelok connection (picture 3.2).

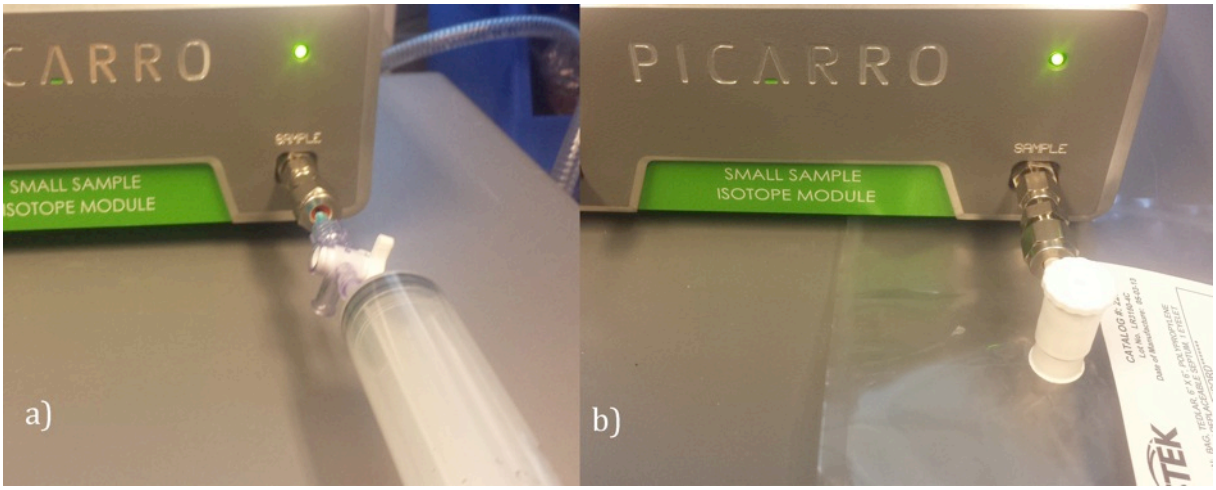

Picture 3.1 – Injection methods that was tested during the initial tests: a) injection method using a syringe through a septum and b) injection method using a tedlar bag.

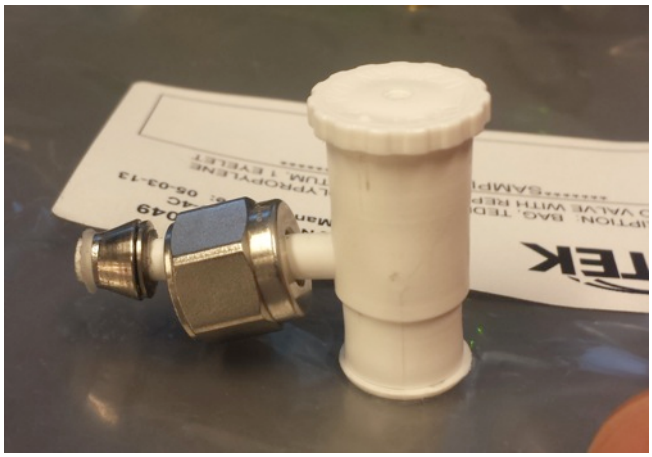

Picture 3.2 the modified tedlar bag used for injection sample into the SSiM

The syringe has the advantage that the sample can be transferred directly from the sample to the SSiM. However, using a syringe requires precise timing when injecting the sample since the SSiM only leaves a couple of seconds to inject the sample before the valves closes. This often resulted in not being able to inject the entire sample into the analyzer - especially if a large sluggish syringe is used. The septum that is used to inject the sample through also needs to be changed every 4-5 measurement and the correct placement and fitting of the septum is critical to avoid air leakage into the system. Using the tedlar bag the vacuum in the SSiM drags in the sample automatically without any manual effort. The sample can also be diluted directly in the bag if needed. The sample needs however to be transferred from the sample bottle to the bag using a syringe.

To determine the most appropriate injection and sample preparation the difference in the Picarro working standard was measured with the both methods.

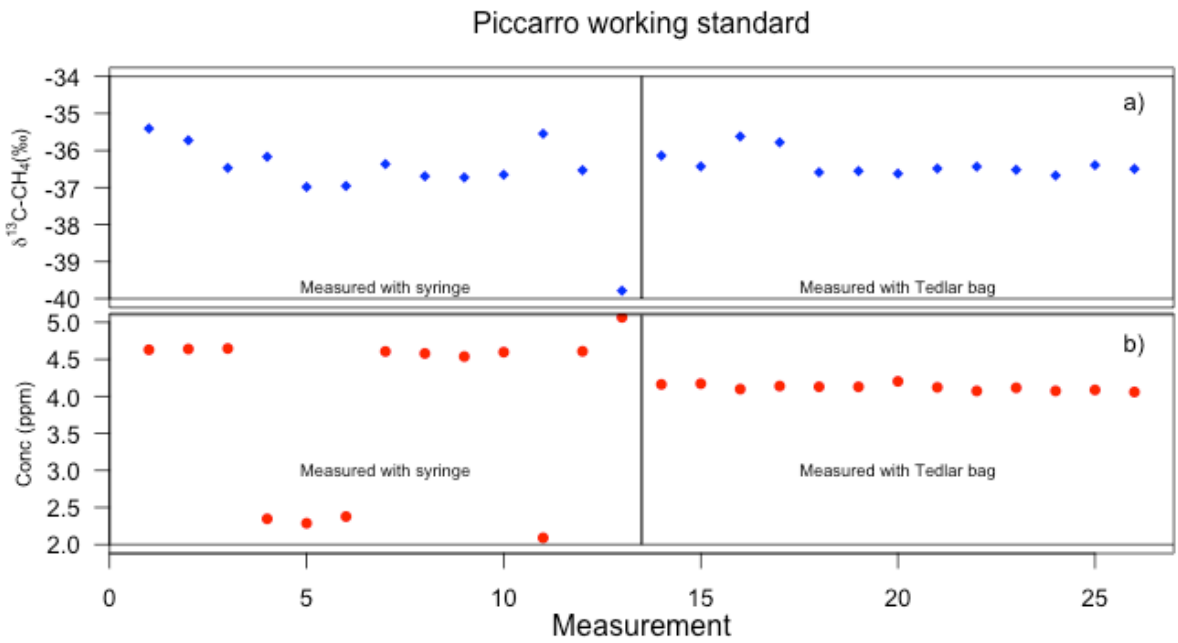

Figure 3.1 the two different injection methods using a syringe and using tedlar bag. a) δ13C-CH_4 in permille and b) concentration in ppm.

Injection method					
Method	**Concentration (ppm)**	**Standard deviation (ppm)**	**δ^{13}C-CH_4 ‰**	**STD δ^{13}C-CH_4**	**n**
Syringe wo outliters	4.35	0.71	-36.30	0.43	9
Syringe w outliers	3.92	1.11	-36.62	1.04	12
Tedlar bag	4.12	0.04	-36.36	0.31	12

Table 3.1 - the mean concentration, standard deviation of the concentration, the isotopic composition and the standard deviation of the isotopic composition for each injection method.

Figure 3.1 shows concentration as well as δ^{13}C-CH_4 of the standard for both injection methods, the results are also summarized in table 3.1 it can be seen in figure 3.1 that there are several outliers in the concentration measurement when using the syringe. This may be an artifact when the timing of the injection was wrong and only a part of the standard was injected. These does not seem to affect the δ^{13}C-CH_4 except for measurement number 12.

Overall the measured δ^{13}C-CH_4 is affected by the change in injection method but not significantly. The concentration (figure 3.1b) though showed that the concentration became more stable when the injection method was changed from syringe to tedlar bag. However, for unknown reasons the concentration of the standard was slightly lower

when the tedlar bag was used. There may be some dead volume in the tedlar bag connection (picture 3.2) that may affect the evacuation or in the entire bag. However, this does not seem to affect the in $\delta^{13}C\text{-}CH_4$ composition significantly therefore is not considered important for the study. Based on the more reproducible results and the user-friendliness, it was decided to use the tedlar bag for this study.

3.2 Stabilization time

When the Picarro is switched on, the instrument needs some time to stabilize before the measurement can considered being accurate. To determine the time of stabilization a 24-hour time series was created measuring the working standard directly after startup. Prior to those measurements the Picarro had been shut down for 1.5 months giving a conservative stabilization time compared to a daily shutdown.

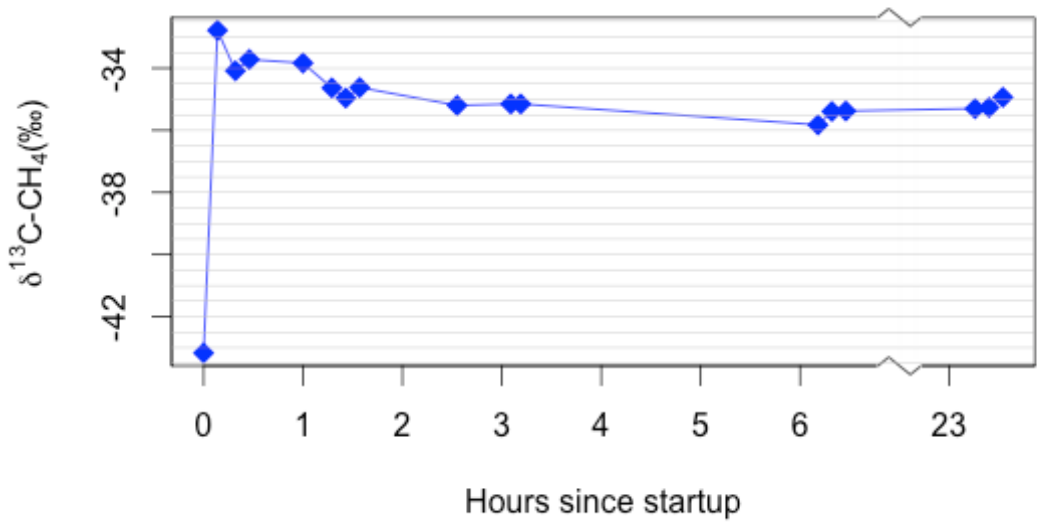

Figure 3.2 - the stabilization time form hour 0 to 24 hours after Picarro start up.

Figure 3.2 shows that immediately after the Picarro was turned on, $\delta^{13}C\text{-}CH_4$ of the working standard is considerable lighter than usual (-43.17‰, the long term mean of the standard being -36.16±0.56‰). The reason for that could be small amounts of air in the SSiM or absorbed to the surfaces of the system. The following measurements show at first heavier than average values. After approximately 3 hours after the start up, the $\delta^{13}C\text{-}CH_4$ stabilized and gets closer to the long-term average.

The results from the stabilization time shows that for best results the system should be running for at least 3 hours prior to measurement. The best is to let it run all the time during the measurement time.

3.3 Reproducibility and long term stability

Measurements were made between October 2015 and March 2016. Figure 4.3a shows the results of all the Picarro working standard measurements performed on the Picarro system during this period. For comparison figure 3.3b shows the GC-IRMS control standard measured on the GC-IRMS over the same time period.

The figure shows that there is no systematic drift in the Picarro. The red stars (figure 3.3a) are where the Picarro cannot be considered stable, based on the stability test (section 3.2). The GC-IRMS measurements (figure 3.3 b) show a visible drift over the measurement period. This drift can also be seen in figure 3.4b where the measurements are plotted on respective date. Whether this variation is based on instrument performance or due to variations in the standard is unclear. Note that the GC-IRMS is calibrated daily while daily calibration of the Picarro was not calibrated during the whole period.

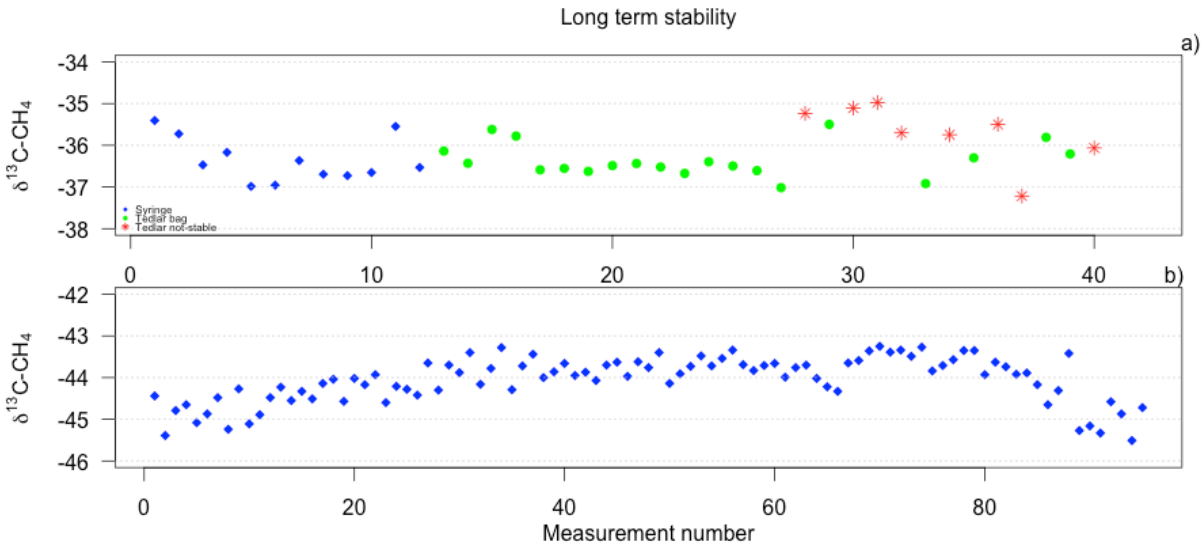

Figure 3.3 the long-term time series of (a) the Picarro working standard with the isotopic composition of the standard on the y-axis and the measurement number on the x-axis. The blue diamonds represents the $\delta^{13}C$-CH_4 measured using syringe as injection method. The green circles represent Picarro measurement using tedlar bag and red start represents the $\delta^{13}C$-CH_4 measured during the stability time. B shows the GC-IRMS control standard measured during the same time span.

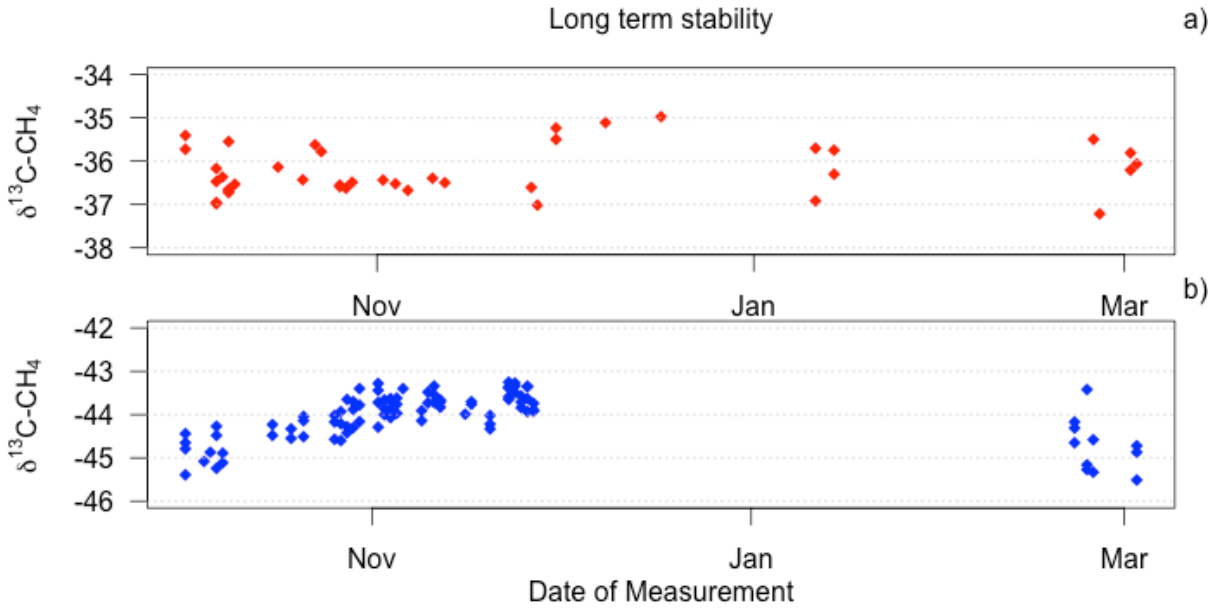

Figure 3.4 the two standards measured on its respective system plotted by date the measurement was performed. A is the Picarro working standard measured on the Picarro system and b is the GC-IRMS control standard measured on the GC-IRMS over the same timeframe.

Long term stability				
System/standard	**Mean $\delta^{13}C$-CH_4 ‰**	**STD $\delta^{13}C$-CH_4 ‰**	**n**	**Error of mean**
Picarro all values	-36.22	0.56	40	0.09
Picarro stable values	-36.35	0.44	32	0.08
GC-IRMS	-44.06	0.55	95	0.06

Table 3.2 the mean $\delta^{13}C$-CH_4 of the Picarro and the GC-IRMS with standard deviation, the number of measurements on each system and error of mean.

Table 3.2 show the $\delta^{13}C$-CH_4 composition of both standards measured on their representative system. Standard deviations of both the systems are comparable. The error of the mean however is larger for the Picarro due to the lower amount of measurements on the Picarro. If this could be improved by more measurements under ideal conditions (tedlar bag, system running continuously) remains to be investigated. The GC-IRMS control standard is measured multiple times during the day that show a variety of daily standard deviation from 0.06‰ to 0.85‰. The Picarro working standard was usually measured once per day resulting in no daily differences.
Based on the results both the systems preforms comparable over a longer period of time. The GC-IRMS has to be calibrated daily while this is not a must on the Picarro system.

3.4 Accuracy

The next step is to investigate how accurate the Picarro measured the standards. This was done by repeatedly measuring both the Picarro working standard and the GC-IRMS control standard on both systems and compare the results (table 3.3).

	Picarro			GC-IRMS		
	$\delta^{13}C$-CH_4 (‰)	STD	n	$\delta^{13}C$-CH_4 (‰)	STD	n
Picarro working standard	-36.35	0.44	32	-39.66	0.47	4
GC-IRMS controll standard	-42.08	0.64	7	-44.06	0.55	95

Table 3.3 - the Picarro working standard and the GC-IRMS control standard measured on the Picarro and the GC-IRMS.

The results do not agree within their respective standard deviations. The difference for the Picarro working standard is 3.44±1.03‰ and for the GC-IRMS control standard the offset is 2.08±1.09‰. The reason for the difference is unclear, but since both differences agree within their standard deviation, the offset could be linear and corrected for. During the later stages of this study the GC-IRMS control standard was sent for external calibration. The system that was used during the external calibration was also a GC-IRMS. The results from the calibration showed a value of -41.42±0.18‰, a value falls close to the standard deviation of the measurements performed on the Picarro. Further investigations are needed before concluding which system shows the most accurate value.

3.5 Concentration dependence of the isotope signal

The Picarro can measure carbon isotopes in two modes, High precision (HP) and High Dynamic Range mode (HR). The HR is designed to measure high concentrations of methane. The HP mode gives best precision on concentration spanning from 1.8ppm to 12ppm. To test the potential influence of the CH_4 concentration within and outside this range a diluted 100ppm CH_4 standard was measured. The concentrations measured ranged from 73ppm down to 0.5ppm.

Concentration drift		
Concentration (ppm)	HP $\delta^{13}C$-CH_4 (‰)	HR δ13C-CH4 (‰)
73.25	8789	-41.32
34.52	-38.97	-40.87
21.30	-40.52	
7.52	-40.89	
4.95	-40.31	
3.52	-40.24	
1.09	-42.03	
0.56	-38.21	

Table 3.4 – A diluted 100ppm methane standard measured on the Picarro to determine the concentration dependence of the $\delta^{13}C$-CH_4 with a methane level above and below the dynamic range of the instrument. The diluted standard was measured one time.

Table 3.4 shows the concentration influence on the isotope signal. In the HP mode, results from a concentration from 21.3 to 3.53ppm fall within the standard reproducibility given in chapter 3.3. For values below 1.8ppm up to 35ppm, a deviation in the isotope value is observed. However, the values are within a range of <5‰. Only the highest concentration of 73ppm, the HP mode measurement is out of the range of what is considered reasonable. This shows that the recommended HP range Picarro gives is reasonable and even a little conservative. Outside the HP range the HR mode gives reasonable results. For best results it is to work in the recommended range and below 20ppm. For high concentration manual sample dilution is needed. In this case samples needs in this case be analyzed on a concentration analyzer (in this study the GC-FID) prior to the isotopic analyze. Below the recommended range the Picarro still gives reasonable results, however with lower precision and accuracy.

3.6 Possible interference effects

Molecules (such as ethane, ethylene, ammonia and compounds containing sulfur) that have absorption spectra close to methane can cause interference to the CH_4 carbon isotope measurement. Helium can give interference by changing the background absorption lines.

For helium and ethane interference was confirmed and proven to be significant. The measurements of gases containing helium and ethane (15 and 150ppm) are shown in table 3.5. As these gases do not affect the GC-IRMS the $\delta^{13}C$-CH_4 values from the GC-IRMS

measurements is here used as a reference. It can be seen that measurements of these gases show significant differences.

Possible interference	Amount	GC-IRMS (‰)	Picarro (‰)
Helium	50% Helium 50% Nitrogen	-36.66	-18.07
Ethane	1ml 150ppm	-40.41	-2.15
Ethane	10ml 15ppm	-39.89	-0.25

Table 3.5 - the interference with Helium and Ethane compared to the $\delta^{13}C$-CH_4 (‰) measured GC-IRMS and Picarro.

A higher concentration of carbon dioxide and H_2O can also give incorrect values on the Picarro if the concentrations are above the dynamic range (for CH_4 12ppm, 4000ppm for CO_2 and 100ppm for H_2O) caused by optical sickness.

Concentration CO_2 (ppm)	$\delta^{13}C$-CH_4 (‰)	STD $\delta^{13}C$-CH_4 (‰)
386.92	-36.53	0.40
997	-36.10	0.07
1185.55	-36.40	0.32
4203.87	-35.83	0.06

Table 3.6 - the interference with an increased concentration of CO_2 and the change in $\delta^{13}C$-CH_4 (‰) with the increased CO_2 concentration.

Table 3.6 shows the effect of an increasing concentration of carbon dioxide that was added to the Picarro working standard. This was tested because higher concentrations of CO_2 are expected to be seen in the real samples. A first significant change in the $\delta^{13}C$-CH_4 values is observed at concentrations above 4000ppm, which that is in agreement to the recommended levels. This effect is however small and cannot be considered significant to the study.

The observed differences show that caution must be taken when using samples that may contain these gases and when choosing a gas to use for a headspace. If a sample is suspected to contain any helium and/or ethane another measurement method is recommended.

3.7 CH_4 concentration measurement – Picarro

The Picarro also gives the CH_4 concentration of the measured gas. The given concentration is however expected to be 2-6% lower than the actual because of a small dilution effect with zero air contained in the SSiM. The concentration of the Picarro

working standard as given by the manufacturer is 5.07±0.1ppm. Figure 3.5 show the measured concentrations of the Picarro working standard. The mean concentration of the Picarro measurement is of 4.05±0.62ppm. This is lower than the given the percentage due to effects of the SSiM.

If the Picarro is to be used for CH_4 concentration measurement, it needs to be calibrated for this offset. In this study additional concentration measurements are anyway preformed with the GC-FID to determine if dilution is needed, so such calibration is not needed.

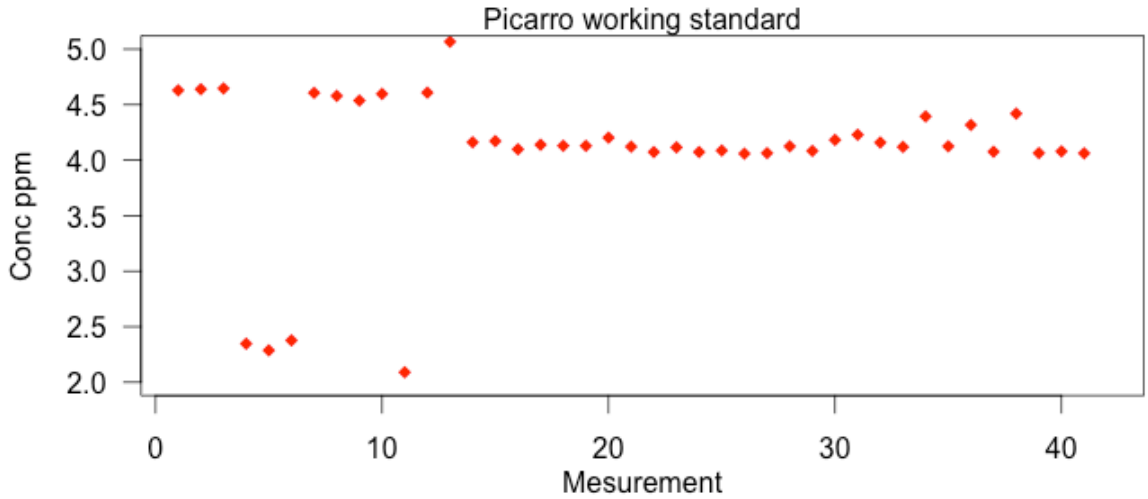

Figure 3.5 the concentration of the Picarro working standard measured over the long term stability time period. The lower values are considered outliers and were measured with a syringe as injection method.

3.8 Conclusion

The Picarro instrument with the SSiM was tested to determine its suitability for discrete measurements. Two injection methods were tested: syringe and tedlar bag. The choice of injection method showed a small effect on the $\delta^{13}C$-CH_4 but not significant. However, the concentration measurement became more stable using a tedlar bag. The standard deviation of both the concentration and $\delta^{13}C$-CH_4 became smaller using a tedlar bag than a syringe. Another advantage of the tedlar bag was that samples could be diluted in the tedlar bag directly and the method is more user friendly.

The stabilization time of the instrument after startup was determined. Based on the results, it is recommended to let the instrument stabilize for 3hours before measurements are performed. The start up of the Picarro is however simple, no

supervision during start up is needed. The system performs best if the system is on continuously.

Long time stability of the system was tested over a course of 6 months using a 5ppm standard (Picarro working standard). No long time drift was observed and the reproducibility of the standard was ±0.56‰. The GC-IRMS control standard was measured on the GC-IRMS over the same time. The GC-IRMS show some drift over the time span but show a comparable reproducibility of ±0.55‰.

Regarding the accuracy of the Picarro measurement with compared to the GC-IRMS. The difference of the Picarro working standard is 3.44±1.03‰ and the GC-IRMS control standard is 2.08±1.09‰. The GC-IRMS control standard was however during the final stages of this study sent for external calibration. The calibration resulted in a value of -41.42±0.18‰. This would minimize the offset between the GC-IRMS control standard and the Picarro measurements. Further investigation of this standard is needed.

The dependence of methane concentration to the $\delta^{13}C$-CH_4 was investigated for a range of concentrations from 73ppm to 0.5ppm. Within the range of 1.8 to 12ppm there is no influence. The results indicate that a concentration above (30ppm) and below (0.5ppm) the HP modes range influence the isotope signal of around 5%. Dilution is recommended for concentrations above 20ppm. Above this concentration the HR mode could give a usable reading. Low concentrations of methane give a significant effect on the results.

The effect of high concentrations of CO_2 and how it affects the $\delta^{13}C$-CH_4 was studied. It shows that the recommendations from Piccaro are accurate; there is a change in the $\delta^{13}C$-CH_4 above a CO_2 concentration of 4000ppm. The effect is however not large (around 2%) but caution must be taken if concentration reaches above this value. Other molecules (such as ethane, ethylene, ammonia and sulfur) that have absorption spectra close to methane can cause interference to CH_4 measurement. Here the interference from ethane could be compared and proven significant. Helium that contaminates the chamber was also proven significant. Caution must though be taken

using an appropriate headspace gas and if samples contain significant levels of these gasses.

The accuracy of the Picarro concentration measurements was determined using the Picarro working standard. The concentration was as expected lowered with an SSiM connected but lower than the 2-6% given by Picarro. If the Picarro is to be used for CH_4 concentration measurements calibration recommended. This was not necessary during this study since the concentration was measured with the GC-FID. The CH_4 concentration measured on the Picarro was only used as a reference.

The Picarro system used during this study still ran on factory calibration showing that the system does not need a frequent calibration. However a more frequent calibration may have improved the results. Calibration of the system may be appropriate when the system have been shut down for a longer period of time. During this study uncertainties in the comparison between the Picarro and GC-IRMS raised when the external calibration showed that the GC-IRMS control standard was closer to the value given by the Picarro. Further investigations of both calibration of the system and the GC-IRMS control standard is needed.

The initial tests showed that the Picarro performs comparable to the standard method of isotope analysis at Stockholm University, the GC-IRMS and can be used as the main method of isotope measurement for this study. Compared to the GC-IRMS it is much more user friendly; once the sample is injected into the analyzer no further supervision is needed. It does not require daily calibration, the system used for this study used the factory calibration, and it does not use any consumables except small amounts of zero air.

4 Pilot experiment – Brunnsviken

After the initial tests showed that the Picarro could be used as a main measurement technique a pilot experiment was conducted. The aims of the pilot experiment were to test the performance of the Picarro on real samples and to evaluate problems and improvements of the incubation method.

The samples for the pilot experiment were acquired from Brunnsviken, an estuary in Stockholm connected to the Baltic Sea. The sample location was chosen for its accessibility (located close to Stockholm and accessible by a small boat)
Sampling was conducted in September 2015 using a Ruttner sampler. The depth of the sampling site was 9.5m and seven depths of the site were sampled for start concentration and isotope measurements. Three depths were chosen to be sampled for time series analysis (2, 5 and 9m). Triplicates for each depth and time point were sampled to get a good statistical reproducibility. In situ measurements of salinity, oxygen and temperature were conducted during the sampling.

4.1 Experimental set up

The incubation study was made at room temperature (roughly at around 20°C) in an attempt make the bacteria oxidize/metabolize at a higher rate. During the time series, methane concentration and $\delta^{13}C$ of three samples were measured once every seven days. Shortly before the analysis, a 30ml headspace was added to the samples (as described in chapter 2.2.1), 5ml was used for concentration analysis on the GC-FID and up to 20ml for $\delta^{13}C$ on the Picarro. A number of the samples were also analyzed with the GC-IRMS for a comparison of the Picarro performance on real samples.

4.2 Starting conditions

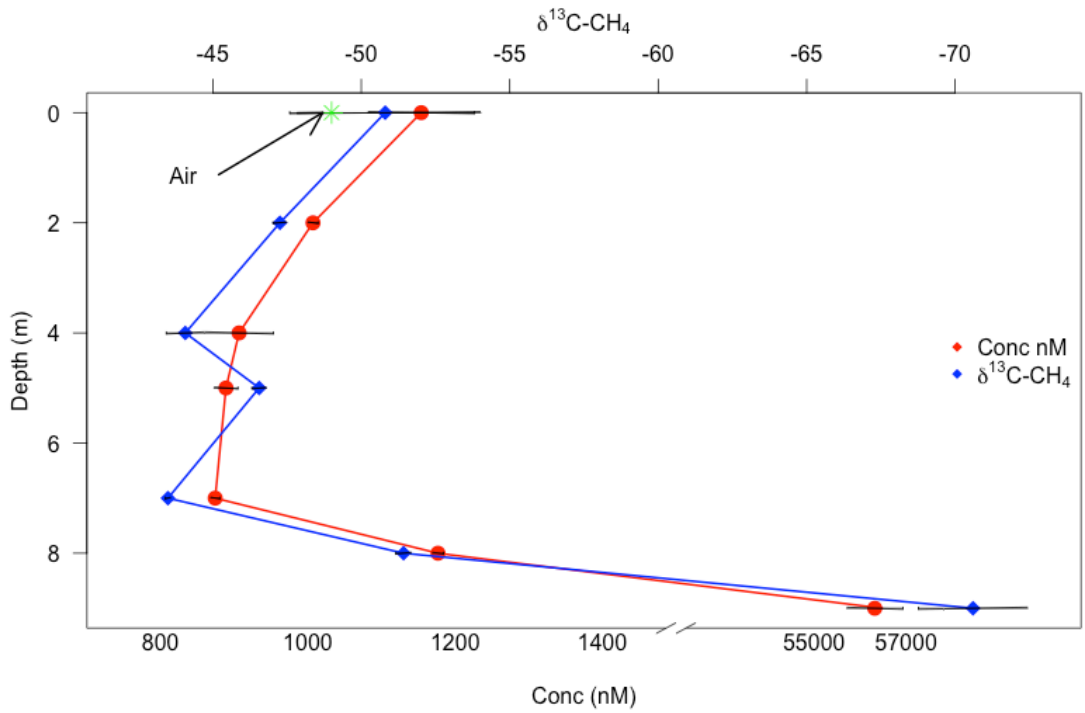

Figure 4.1 – Methane profile of Brunnsviken with concentration (nM) shown as red circles. $\delta^{13}C$-CH_4 (‰)as blue diamonds.

Figure 4.1 shows the dissolved methane concentration and isotopic composition from the water column in Brunnsviken. The concentration is highest in the bottom (8 and 9m) and lowest concentration in the pelagic water of 7m (table 4.6). From 7m on, an increase in the concentration towards the surface water is observed with a second maximum at 0m. The $\delta^{13}C$-CH_4 shows a similar pattern as the concentration with light $\delta^{13}C$-CH_4 the most depleted $\delta^{13}C$-CH_4 in the in the depths of 8 and 9m. After getting heavier at 7m the methane becomes depleted again towards the surface reaching an isotopic signature of -50‰ at the surface water.

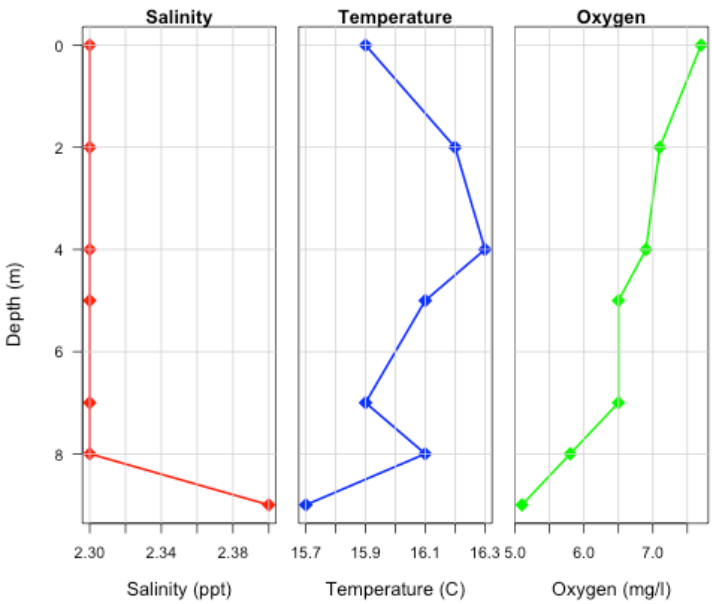

Figure 4.2 - the physical properties of Brunnsviken with salinity, temperature and oxygen.

The physical properties of the water column at Brunnsviken sampling site are shown in figure 4.2. The overall observation from the profile is that there are only small variations with depth. The water shows weak thermal stratification in the top 2m and thermal and salinity stratification in the 2m most bottom. This cannot be used to explain the methane profile in figure 4.1.

4.3 Experimental results – GC-IRMS vs Picarro

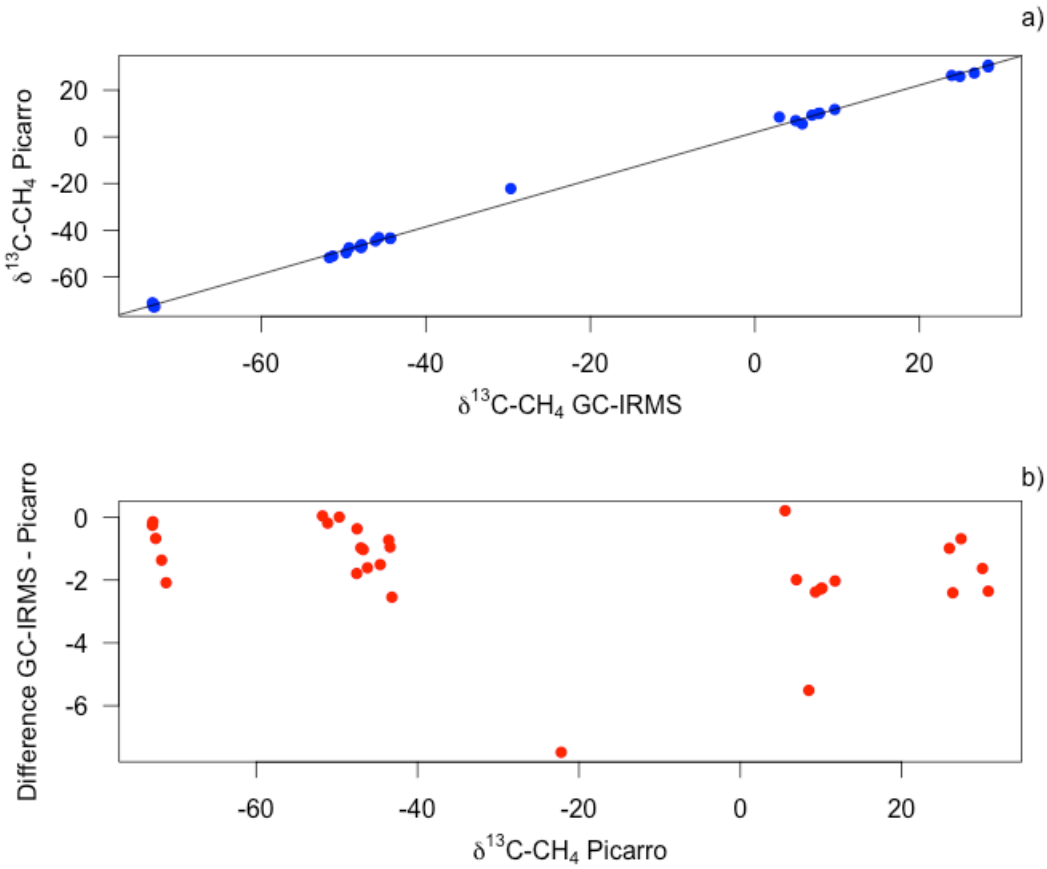

Figure 4.3 the difference in the $\delta^{13}C$-CH_4 measured on the GC-IRMS and on the Picarro using the samples from Brunnsviken. A is the linearity between the GC-IRMS and the Picarro. B is the difference between the GC-IRMS and the Picarro with the measured isotopic composition of the Picarro on the x-axis,

A selected number of samples were measured on both the Picarro and the GC-IRMS. Figure 4.3a show the linearity between the GC-IRMS and the Picarro. The R^2 value was 0.998, which must be considered a very linear relationship.

Figure 4.3b shows the results with the $\delta^{13}C$-CH_4 of the samples measured on the Picarro on the x-axis. The mean of the study was -1.59±1.5‰ with the two outliers. Without the outliers the mean is -1.25±0.86. This strengthens the decision of using the Picarro as the main method of isotope measurement during the study.

4.4 Experimental results – incubation time series

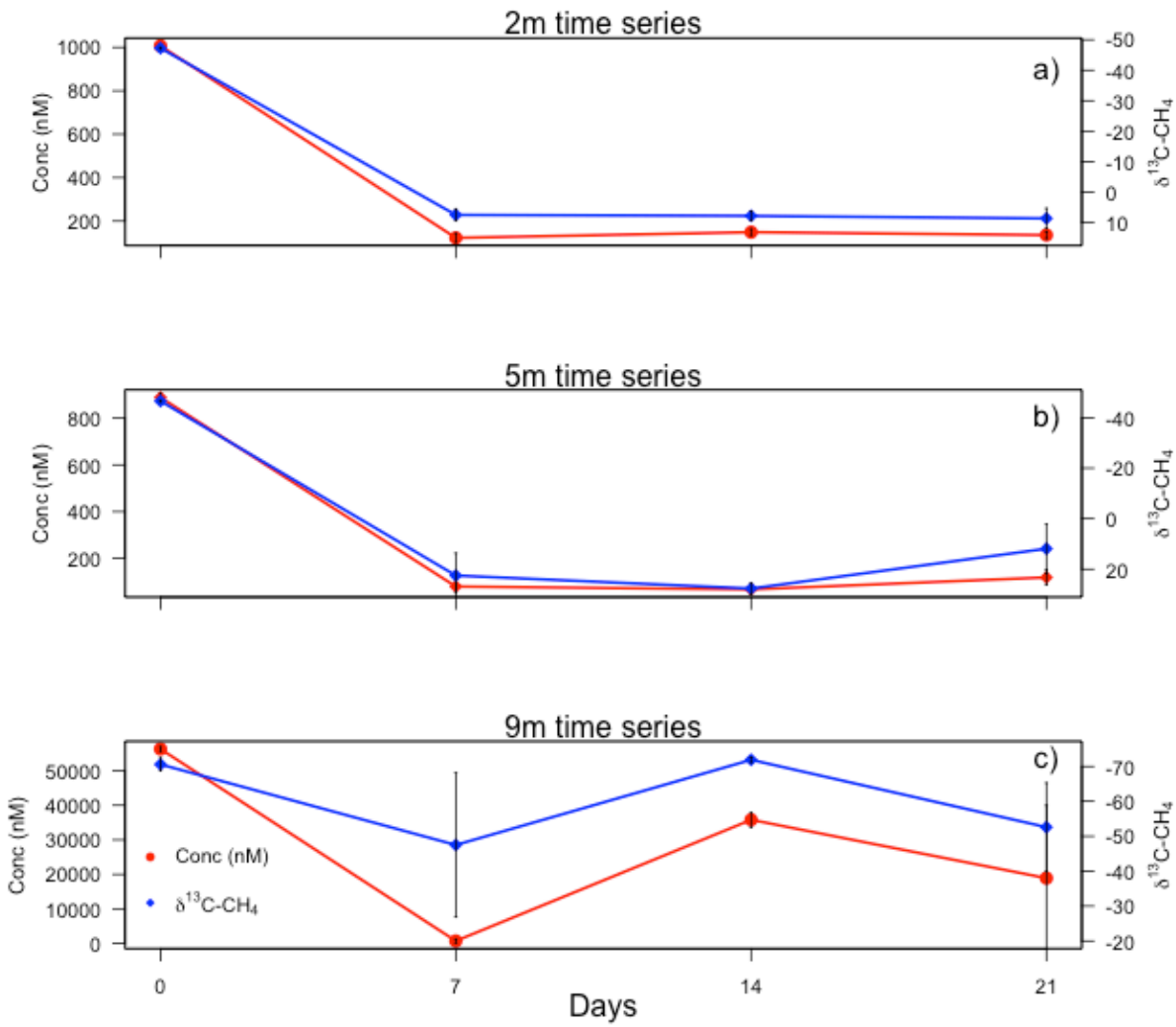

Figure 4.4 - the time series of the three sampled depths where blue diamonds represents the $\delta^{13}C$-CH_4 (‰) and the red circles shows the concentration (nM).

The results from the incubation time series are shown in figure 4.4. The 2 and 5m time series (figure 4.4 a and b) show a similar pattern with a strong decrease in concentration as well as a shift in the $\delta^{13}C$-CH_4 towards heavier values, consistent with methane oxidation. The largest change occurs in the first 7 days, after that there are no significant changes in both the isotope signal and concentration. The 2m time series show a decrease of 90% in concentration and a change in $\delta^{13}C$-CH_4 of 56‰ in seven days. The 5m time series decreases with 90% in concentration and the isotopes shift with 69‰ within the same timeframe. The rate of oxidation is for the first 7 days is 126nM/day for 2m and 115nM/day for 5m.

Figure 4.4c show the 9m time series. This depth shows a different pattern from the other depths. There is no clear decrease in concentration or isotope enrichment during the time series, but rather fluctuation between enriched/depleted isotope signatures and lower and higher concentrations. The variation between the triplicates for each time point is also significantly larger than the other depths. If oxidation occurs in the samples or if it is hidden by strong variations is unclear from the time series plot. The oxidation rate for the first 7days is 7944nM/day and between 14 and 21 days are 2415nM/day.

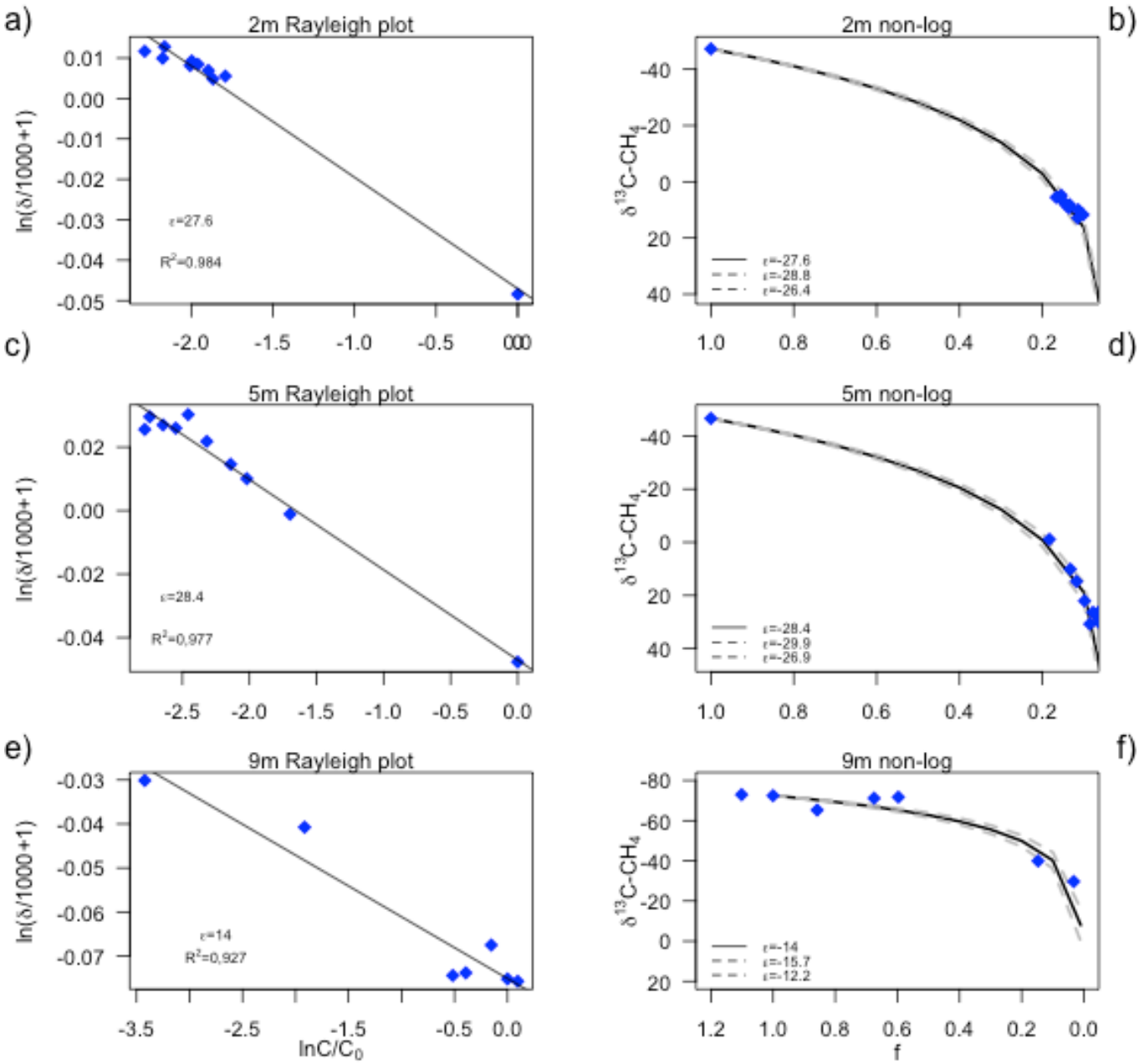

Figure 4.5 the Rayleigh and non-logarithmic curves for 2m, 5m and 9m.

Figure 4.5 (a, c, e) shows the Rayleigh curves for the three sampled depths using the double log plot (described in section 3.1) with linear regression lines. Using the isotopic fractionation factor (ε) calculated from the Rayleigh distillation curves non-logarithmic plots were made for each depth (b, d, f). Two additional curves were created using the error of the slope from the double logarithmic Rayleigh curves.

The depths of 2 and 5m show a linear fit that indicate Rayleigh behavior and all have R^2 values greater than 0.9, which is considered a good linear relationship. The isotopic fractionation factors for these depths are 27.6 and 28.4‰. The non-logarithmic curves show the start and the low end of the curve where <20% of the CH_4 is left. The middle of the oxidation sequence is missing, however the fit is appropriate.

9m depth looks like it follows a Rayleigh behavior however, the time series analysis does not. The measured values on the non-logarithmic plot (figure 4.5f) shows more scattered values across line that is larger than the error in epsilon. The remaining methane factor covers more of the line than the other depths. The lower isotopic fractionation factor indicates that there might be more processes than oxidation at the depth. A single value shows a higher f than the assumed start concentration. If this is because of a higher concentration in that sample than the assumed start concentration or if methane has been formed in the sample is unclear.

4.5 Discussion Brunnsviken

4.5.1 Starting conditions

The high methane concentration at 9m of depth indicated that the methane originates from the sediment. The isotopic signature at this depth is also most representative for the source. Based on the $\delta^{13}C$-CH_4 signature of the bottom water methane indicates a methane formation from a microbial source by CO_2 reduction (Whiticar et al., 1986, Whiticar, 1999). The overlaying water shows a lower concentration and methane enriched in ^{13}C that could originate from oxidation or mixing. The surface water shows a signature comparable close (within the standard deviation) to air however the

concentration shows that the water is not in equilibrium with the air (approximately 1.9ppm=4nM). The water column at the sampling site shows little stratification and can be considered well mixed except in the bottom water and cannot help explain the methane/isotope profile (figure 4.2). Since the entire water column is oxygenated aerobic oxidation is expected. The concentrations of the water column are elevated and can be compared to bottom water of previous studies conducted in the Baltic Sea (Jakobs et al. 2013).

The reason for the high methane concentration in the surface can have multiple explanations. One of these could be that methane bubbles are released from sediment and rise quickly up the water column and often escapes oxidation and dissolution (McGinnis et al., 2006). There is the possibility that during sampling bubbles were caught in the sampler at some depths. However, if a bubble was caught in the sampler not only would the concentration be elevated but the isotopic signature of the sediment methane would be retained. The other explanation for the high concentration in the surface water is that methane is formed in the oxygen rich waters. This does not support the prevailing paradigm that methane is only formed in anoxic waters and sediment. However this has been well documented by previous studies such as Grossart et al., (2011) and Tang et al. (2015). Even though the $\delta^{13}C$-CH_4 signal does not show a formation signature this could indicate that the surface water is a mixture of oxidized pelagic water, air signal and the production in the surface waters. Another possibility for the isotope signal is that the methane forming organisms does not fractionate as in the same range as more known methanogenic archea.

4.5.2 Experimental discussion – incubation time series

Depth (m)	Start concentration	Total days	$\varepsilon_{methane}$	Oxidation rate (nM/day)
2	1007	21	27.6	126
5	889	21	28.4	115
9	56318	21	14.0	7944

Table 4.1 – The results from the time series analysis in Brunnsviken

The results of the time series are summarized in table 4.1.

The experiment shows clear signs of oxidation at 2 and 5m depth.

The speed of the oxidation was quicker than expected and can be considered fast compared to other studies (Coleman et al., 1981; Seifert et al. 2006). In 7 days the concentration has decreased significantly in the 2m and 5m samples, with only around 10% of the start concentration remaining. During this time period the isotopic composition have shifted from -47‰ (2m) and -46‰ (5m) to heavier values for both depths. Even positive $\delta^{13}C$-CH_4 values are observed, which is rather uncommon, but has been seen in previous incubation studies such as Coleman et al. (1981). After the first seven days in the time series the oxidation at 2 and 5m seems to halt; the remaining time points show little change in both concentration and $\delta^{13}C$-CH_4. The remaining methane may have become unattractive for the methanotrophic community as discussed by Whiticar et al., (1986) or the bacteria died during the study.

All of the depths in the time series can be fitted linear with high R^2 values indicating a good fit. The 2 and 5m exhibit closed system Rayleigh behavior and can be considered closed systems. The isotopic fractionation of these two depths is very similar and is within the standard deviation of each other. The mean of the isotopic fractionation is 28±0.4‰, which is comparable to previous laboratory studies, from example Coleman et al. (1981) and Feisthauer et al. (2010). The non-logarithmic figures for 2 and 5m show a good fit to the calculated isotopic fractionation factor and the residual methane shows that 10% of the methane remains.

The 9m depth time series does not show the same pattern as 2 and 5m. Samples at each time point show a large variation in both concentration and $\delta^{13}C$-CH_4. From the time series alone it is not clear if there is oxidation in the samples. The values fit nicely to on a Rayleigh curve and the epsilon value could be determined with high certainty as indicated by a high R^2 value that is above 0.9. The calculated fractionation is 14.0±1.8‰ which also matches the values from previous laboratory studies. The error of the slope is however higher at this depth but cannot be considered significant. Here the assumption that the variation between the samples is large in the start conditions of this depth. The triplicate samples measured for the start concentration did not give a represented picture of the variation. This depth is also closest to the source, which could mean that a mixture of isotopically different sources could be present. Another possibility is that the methane present in the bottom water is in different oxidation

stages from the same source. This would mean that already oxidized methane could have been sampled from the start in some bottles. This could be the reason why it does not fit well on the Rayleigh curve. Explanation for the low ε, assuming oxidation, could be that the concentration of the samples is so high that the concentration during the time span of this experiment did not reach the point where fractionation becomes significant (Whiticar and Faber, 1986). The speed of the oxidation that is close to 8000nM/day the first 7 days may also explain the low fractionation factor and indicate that the oxidation rate will influence the isotopic fractionation. The non-logarithmic figure show however that the measured values do not fit the calculated isotopic fractionation. This could indicate that the calculated ε show the mean of the fractionation.

4.6 Conclusion pilot experiment

The pilot experiment at Brunnsviken shows that the tested incubation method can be used to study CH_4 oxidation. There is a significant shift in the isotopic composition towards heavier $\delta^{13}C$ isotopes as well as a decrease in the concentration that together are signs of oxidation. For 2 and 5m the change in isotopes and concentration stops after the first time point. During the incubation experiment the shift towards heavier $\delta^{13}C$ isotopes is very strong and results in positive carbon isotopes values at the depth of 2 and 5m. At 9m the measurements is more scattered and if oxidation occurs in the samples is unclear. Some samples looked oxidized while other does not. The Picarro preformed well using real samples compared to the GC-IRMS and strengthens the decision to use the Picarro as the main measurement technique.

The conclusions of the pilot experiment are that the incubation method can be used for oxidation experiment and that the oxidation is faster than previously expected. Having a higher precision of the start concentrations could give a more precise insight in the oxidation.

5 Main experiment - East Siberian shelf

After the pilot experiment the main experiment was initiated aiming to investigate the methane oxidation in the East Siberian shelf. This was done by setting up a number of sub-experiments with different parameters. To investigate the presence of water column oxidation an experiment containing only water from the Siberian shelf was performed. In this experiment two different parameters (temperature and concentration) were changed to see if it affects the oxidation. In the second sub-experiment a small amount of sediment was added to the water to see if it can affect the oxidation. This experiment was also performed at two different temperatures (4°C and 20°C).

The sampling of the water from the Siberian sea was conducted during the SWERUS expedition in the summer of 2014. The sampling site of the water used in this experiment was sampled at 73 24'N and 176 31' E (figure 5.1). The sampling depth of the water was 8m.

The sediment used in the experiment was acquired at station 23 at 76° 17.05'N and 129° 34'E (figure 5.1). The depth of the sediment is 0-2cm below sea floor. The water depth at station 23 is 54m and the surface temperature of the sediment was 4-5°C.

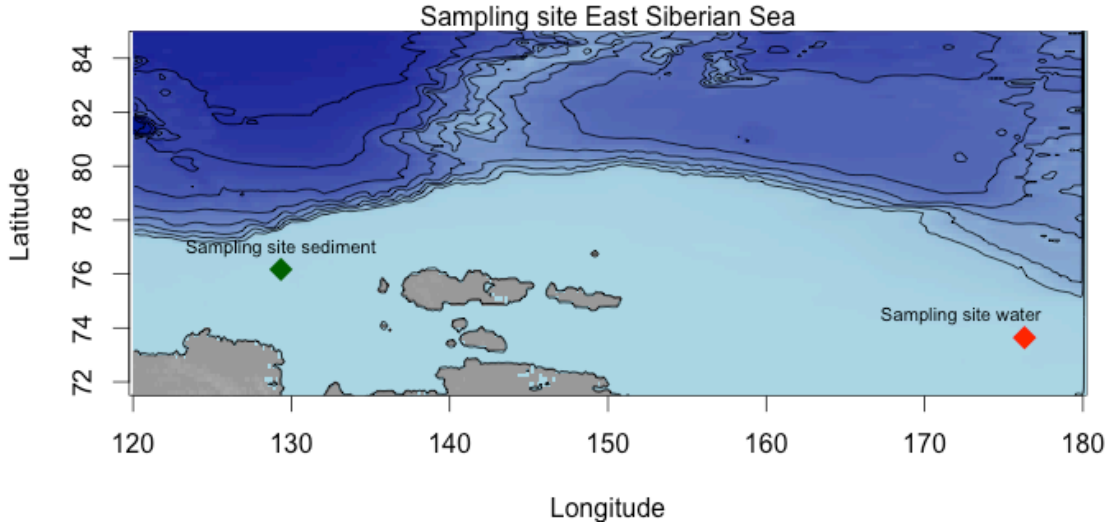

Figure 5.1 – the sampling site of sediment (green diamond) and water (red diamond) in the East Siberian Sea.

5.1 Experimental set up

The water obtained from the SWERUS expedition had been frozen since the expedition and the methane concentration in the water is negligible (possibly due to low starting concentration, oxidation or loss to atmosphere). Therefore a known concentration of methane standard gas was dissolved in the samples. This gave the opportunity to create a more reproducible starting condition for both the concentration and the $\delta^{13}C$-CH_4 than the pilot experiment. This way the water served more as a matrix containing a potential methane-oxidizing community.

The same procedure was used for the sediment samples except that 0.5ml of sediment was added to the serum bottles before the water was added.

Experiment no	Water/Sediment	Incuation temperature	Start concentration (nM)	Standard deviation (nM)
1	W	20°C	59.88	1.22
2	W	20°C	664.67	6.45
3	W	4°C	508.92	44.55
4	W/S	20°C	448.75	31.10
5	W/S	4°C	427.285	27.35

Table 5.1 – the matrix of the experiments conducted with water and sediment from the East Siberian Shelf.

5.1.1 Incubation

As with the pilot experiment three of the samples were measured for start concentration and isotopic composition to determine the variation between bottles. For the time series, only one bottle was measured at each time point since the pilot experiment showed that variation between sampled at one time point is likely to be small. This variation was expected to be even lower using an artificial methane concentration and isotope composition. Concentration and isotopic composition measurements were at first performed every week but later the time between each measurement was extended due to much slower oxidation than in the pilot experiment.

As for the pilot experiment a 30ml nitrogen headspace was introduced prior to the analysis as described in chapter 2.2.1. The analysis of the samples was performed on the GC-FID (methane concentration) and the Picarro analyzer ($\delta^{13}C$-CH_4).

5.2 Experimental results

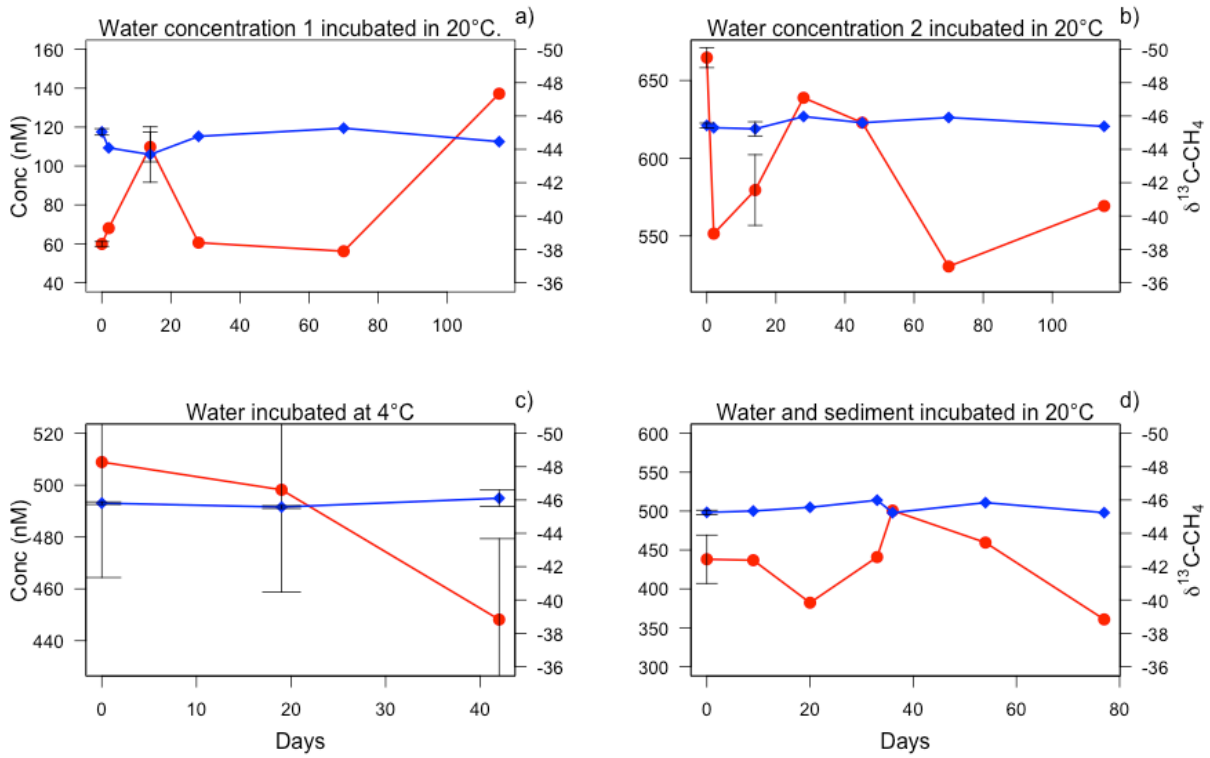

Figure 5.2 – the time series of experiment 1 to 4 where the $\delta^{13}C$-CH_4 is shown as blue diamonds and the concentration is shown as red circles.

The time series of experiment 1 to 4 are shown in figure 5.2. All of the experiments show a variation in concentration throughout the time series. The $\delta^{13}C$-CH_4 in all the experiments is however stable (within the measurement precision) and does not show a significant change during the time of the experiments. The concentration measured on the Picarro (not shown here) show a significant variation indicating that the concentration varies is not due to measurement error on the GC-IRMS, rather concentration differences between bottles.

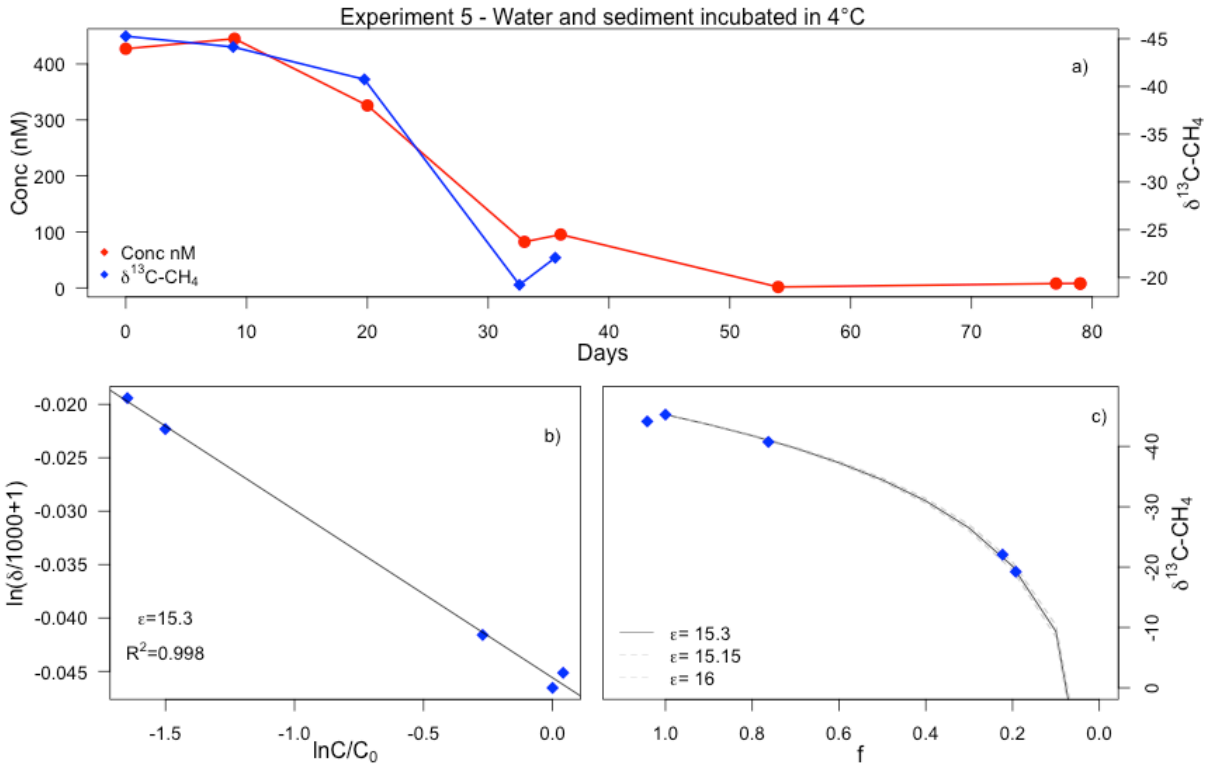

Figure 5.3 the results from experiment 5 where a) is the time series of the experiment, b) the double logarithmic Rayleigh curve and c) is the non-logarithmic curve.

The results from experiment 5 (water and sediment is incubated in 4°C) are shown in figure 5.3. Figure 5.3a shows time series of the concentration and $\delta^{13}C$-CH_4 of the time series. In contrast to the other experiments, here a clear trend towards lower concentration and enrichment in in the $\delta^{13}C$-CH_4 can be seen - indicating oxidation. The oxidation rate between time point 2 and 3 is 19nM/day with a decrease in $\delta^{13}C$-CH_4 21‰ during this time period. From time point 4 the concentration became too low get reliable isotope measurements on the Picarro (below <0.5ppm). Figure 6.3b show the double-logarithmic Rayleigh curve created from the time series. The linear fit of the values gives an R^2 very close to 1 and an isotopic fractionation factor of ε=15.3±0.15‰.

Figure 6.3c show the non-logarithmic curve created using the calculated ε. All the measured values follow the line in a fashion that can be described as oxidation.

5.3 Discussion

5.3.1 Time series – oxidation

The results from the experiment are summarized in table 5.2.

In experiment 1 and 2 there is a variation in the concentration that is larger than the standard deviation during the time series that show both increasing and decreasing values from the start concentration. The isotopic composition is however constant indicating that there is no methane formation or oxidation in the samples. Experiment 3 shows a decrease in concentration at the final time point that could indicate the first stage of oxidation. However the decrease is within the standard deviation between the samples and oxidation is uncertain.

Experiment 4 does not show any direct signs of oxidation. From time point 4 on, the concentration is continuously decreasing, however the isotopes show no indication of a shift towards heavier $\delta^{13}C\text{-}CH_4$ values and the concentration of the final sample is within the range of the start concentration. Whether or not this is a sign of oxidation or measurement error/spread between samples is unclear.

Experiment no	Water/Sediment	Incubation temperature	Start Concentration (nM)	Oxidation	Total days
1	W	20°C	60	Not detected	115
2	W	20°C	665	Not detected	115
3	W	4°C	509	Uncertain	42
4	W/S	20°C	449	Uncertain	77
5	W/S	4°C	427	Yes	79

Table 5.2 - the summarization of the experiments conducted on the East Siberian Shelf

Experiment 5 (the samples containing sediment and that were incubated in a 4°C environment) show a decrease in concentration as well as an enrichment of $\delta^{13}C\text{-}CH_4$ that indicate oxidation. Even if the methane concentration after the fourth time point became too low to measure accurate $\delta^{13}C\text{-}CH_4$ on the Picarro, the trend up to that time points toward clear signs of oxidation. This indicates that the microbial consortia present in the sediment are only capable of efficiently oxidizing methane when the

temperature is low. The oxidation rate of experiment 5 was calculated to be 19nM/day and the isotopic fractionation of ε=15.3±0.15‰ (table 5.3), that is in the low end of previous laboratory experiments such as Coleman et al. (1981) and Feisthauer et al. (2010) but also in the range of field studies such as Damm et al (2007). The close fit of the Rayleigh plot indicates a closed system Rayleigh behavior. The residual methane model show that the last measureable sample of experiment 5 shows an f-value close to 0.2, however the concentration of the samples after this time point show that the oxidation presumably continued.

Experiment no	Water/Sediment	Incuation temperature	Start concentration (nM)	Total days	$\varepsilon_{methane}$	Oxidation rate (nM/day)
5	W/S	4°C	427	79	15.3	19

Table 5.3 – Summary of experiment 5

The lack of oxidation in the water column can have multiple explanations, for example. (1) The water lacks or has small communities of methanotrophic bacteria. The sampling depth of 8m may be above the oxidation zone in the water column (as discussed by Jacobs et al (2013) and Shubert et al. (2006)). (2) The water sampling and storage may have been subjected the methanotrophic community to extreme conditions that may have killed the methanotrophic bacteria. (3) The oxidation rates might be extremely slow, so time span of the experiment was too short to see any signs of oxidation. An estimation of the oxidation rate on the East Siberian Shelf was made by Shakhova et al., (2015) which would be a decrease by approximately 10nM for the experiments containing only water. The oxidation rate according to their study was 0.1nM/day in the water column.

Possibilities that experiment 5 shows signs of oxidation could be that (1) sediment contains a higher concentration of methanotrophic bacteria or (2) that the microbial community consists of psychrophilic consortia. Psychrophilic consortia have been a research subject in the tundra permafrost in Siberia. Studies by for example Trosenko and Khmelenina (2005) and Omelchenko et al. (1993) found that specialized microbial communities in the permafrost show most activity in colder environments from -5°C up to +7°C. Both of these studies were conducted in terrestrial permafrost. Presence of marine psychrophilic consortia in the Artic is very likely.

What the microbial community in the sediment of the sampling site consist of is unclear at the moment and further investigations of the sediment are needed. However, this study indicates that there are no microbial communities that are able to oxidize under higher temperatures present in neither sediment nor water column.

6 Conclusion and outlook

In this study the methane oxidation on the East Siberian Shelf was investigated. The kinetic isotope effect was determined from CH_4 concentration and $\delta^{13}C$-CH_4.
First the measurement method for $\delta^{13}C$-CH_4 using a CRDS analyzer from Picarro was set up and tested. The incubation method was tested using a pilot experiment with samples from a small estuary close to Stockholm (Brunnsviken). The main incubation experiment with samples from the East Siberian Shelf was designed based on the results from the pilot experiment.

The precision of the Picarro compared to the GC-IRMS was from 2.08±1.09‰ to 3.44±1.03‰ using different standards. Based on the overall performance of the Picarro, that proved comparable to the GC-IRMS and its user-friendliness compared to the GC-IRMS was used as the main measurement technique for $\delta^{13}C$-CH_4 during this study.

The pilot experiment showed clear signs of oxidation, indicating that the method worked. The samples from 2 and 5m showed similar oxidation rates, 126nM/day for 2m and 115nM/day for 5m, and isotopic fractionation of 28±0.4‰. The depth of 9m showed an isotopic fractionation 14.8±1.8‰. However, signs of oxidation at 9m are not as clear as the other depths and the samples could be a mix of different oxidation stages.

During the main experiment with samples from the East Siberian Shelf a change in set up was made. A decision to use artificial samples with different parameters was made. A methane standard was used to increase the CH_4 to a known concentration. The samples were also incubated under different temperatures. This experiment showed that was negligible oxidation in the water column at 20°C, but very active oxidation in water mixed with sediment that had been incubated at 4°C. The water/sediment incubated in

4°C environment showed Rayleigh behavior with an isotopic fractionation of 15.3±0.15‰. This is likely because more bacteria is present in the sediment than in the water and that the bacteria present are only able to oxidize methane under cold conditions.

The experiment on the East Siberian Shelf show that there are only psychrophilic bacterial communities present in the sediment and that the oxidation in the water column may be to slow to measure with this method. It shows that that the top 2 cm in the sediment contains methanotrophic bacteria. This could in theory mean that all the water that comes into contact with the top sediment may be subjected to oxidation; the entire shelf could act as a sink for methane. Based on the results of this study all the methane available may be oxidized in a matter of around 80 days down to levels where conventional methods (GC-FID) does not give a result.

When comparing the results from the pilot experiment and the main experiment one must keep in mind that they are totally different systems. Brunnsviken with a maximum depth of 9m showed no chemocline and based on the elevated methane levels a high input of organic material are available for methane production. While the sampling site for the water from East Siberian Shelf was much deeper and probably showed a chemocline and a lower input of organic material, making the oxidation much slower than Brunnsviken. This can be seen in the oxidation rate between the two systems. In Brunnsviken the oxidation rate was calculated to be from 100nM/day to 8000nM/day while the oxidation rate for water and sediment from the East Siberian Shelf was a mere 19nM/day.

Further investigations of both the sediment and water from the East Siberian Shelf are critical to fully understand the processes active.

6.1 Possible improvements

Using a natural sample there is no possibility to know the start concentration of each sample making it hard to determine if oxidation occurs or if a sample contains a different concentration and isotopic composition than another sample. One way to

improve this error is to use one bottle for an entire time series. This however was not practical during this study since the Picarro needs up to 20ml for one measurement meaning that the headspace will change in concentration when a sample is withdrawn. Therefore an artificial sample was used during the main experiment where the assumption that all the samples contain more or less the same concentration of methane.

The choice of sampling depth was proven critical to this experiment. The sampling depth of 9m in Brunnsviken was proven not optimal since the natural conditions were more complex. Neither was the sampling depth at the East Siberian Shelf optimal since the absence of oxidation may be linked to the water depth and that more bacteria may be present in the bottom waters.

The lack of oxidation may also be linked to the decision taken to freeze the water after the cruse. After this study the results showed that oxidation occurred only in cold condition the bacteria might have been kept dormant if the water was kept in a warm environment. This could however have killed or altered the bacterial community.

To be able to tell more precise what processes are active the isotopic composition of hydrogen isotopes should have been used. This however would have required a larger headspace that would not have been practical during this study.
The time frame of this time series may have been to short for oxidation to show in both concentration and isotopes using samples from the East Siberian Shelf. However, a longer time frame is not possible for a masters-thesis.

7 Acknowledgements

I would like to express my gratitude to my supervisors Volker Brüchert for the guidance and support during this project and to Julia Steinbach for all generous support and help. Not to forget the good and fun ideas on how to battle the questions that rose during the initial test and introducing me to R. I would also like to thank Jayne Rattray for answering all the questions about the GC-FID. A big thanks to Magnus Mörth and

Christoph Humborg for letting me use the Picarro and Marc Geibel for showing me how to use it. Special thanks to the SWERUS scientists and crew for the material used in this thesis. I would also like to acknowledge Rienk Smittenberg for lending out his boat, Max Holmström for his good comments on the draft, Sofia Isaksson for her general support and all the people I met during the years at Stockholms Univeristy (no one mentioned, no one forgotten).

8 References

Anisimov, O.A., D.G. Vaughan, T.V. Callaghan, C. Furgal, H. Marchant, T.D. Prowse, H. Vilhjálmsson and J.E. Walsh, 2007: *Polar regions (Arctic and Antarctic).* Climate Change 2007: Impacts, Adaptation and Vulnerability. Contribution of Working Group II to the Fourth Assessment Report of the Intergovernmental Panel on Climate Change, M.L. Parry, O.F. Canziani, J.P. Palutikof, P.J. van der Linden and C.E. Hanson, Eds., Cambridge University Press, Cambridge, 653-685.

Cavity Ring-Down Spectroscopy (CRDS) | Picarro. (2016). [online] Picarro.com. Available at: http://www.picarro.com/technology/cavity_ring_down_spectroscopy [Accessed 8 Mar. 2016].

Ciais, P., C. Sabine, G. Bala, L. Bopp, V. Brovkin, J. Canadell, A. Chhabra, R. DeFries, J. Galloway, M. Heimann, C. Jones, C. Le Quéré, R.B. Myneni, S. Piao and P. Thornton, 2013: Carbon and Other Biogeochemical Cycles. In: *Climate Change 2013: The Physical Science Basis. Contribution of Working Group I to the Fifth Assessment Report of the Intergovernmental Panel on Climate Change* [Stocker, T.F., D. Qin, G.-K. Plattner, M. Tignor, S.K. Allen, J. Boschung, A. Nauels, Y. Xia, V. Bex and P.M. Midgley (eds.)]. Cambridge University Press, Cambridge, United Kingdom and New York, NY, USA.

Coleman, D. D., Risatti, J. B., & Schoell, M. (1981). Fractionation of carbon and hydrogen isotopes by methane oxidizing bacteria. *Geochimica Cosmochimica Acta*, *45*, 1033–1037.

Collins, M., R. Knutti, J. Arblaster, J.-L. Dufresne, T. Fichefet, P. Friedlingstein, X. Gao, W.J. Gutowski, T. Johns, G. Krinner, M. Shongwe, C. Tebaldi, A.J. Weaver and M. Wehner, 2013: Long-term Climate Change: Projections, Commitments and Irreversibility. In: *Climate Change 2013: The Physical Science Basis. Contribution of Working Group I to the Fifth Assessment Report of the Intergovernmental Panel on Climate Change* [Stocker, T.F., D. Qin, G.-K. Plattner, M. Tignor, S.K. Allen, J. Boschung, A. Nauels, Y. Xia, V. Bex and P.M.

Midgley (eds.)]. Cambridge University Press, Cambridge, United Kingdom and New York, NY, USA.

Conrad, R. (2005). Quantification of methanogenic pathways using stable carbon isotopic signatures: A review and a proposal. *Organic Geochemistry*, *36*(5), 739–752. doi:10.1016/j.orggeochem.2004.09.006

Coplen, T. B. (2011). Guidelines and recommended terms for expression of stable-isotope-ratio and gas-ratio measurement results. *Rapid Communications in Mass Spectrometry*, *25*(17), 2538–2560. http://doi.org/10.1002/rcm.5129

Cowen, J. P., Wen, X., & Popp, B. N. (2002). Methane in aging hydrothermal plumes. *Geochimica et Cosmochimica Acta*, *66*(20), 3563–3571. http://doi.org/10.1016/S0016-7037(02)00975-4

Crosson, E. R. (2008). A cavity ring-down analyzer for measuring atmospheric levels of methane, carbon dioxide, and water vapor. *Applied Physics B: Lasers and Optics*, *92*(3 SPECIAL ISSUE), 403–408. doi:10.1007/s00340-008-3135-y

Damm, E., Schauer, U., Rudels, B., & Haas, C. (2007). Excess of bottom-released methane in an Arctic shelf sea polynya in winter. *Continental Shelf Research*, *27*(12), 1692–1701. http://doi.org/10.1016/j.csr.2007.02.003

Dlugokencky, E. J., Nisbet, E. G., Fisher, R., & Lowry, D. (2011). Global atmospheric methane: budget, changes and dangers. *Philosophical Transactions. Series A, Mathematical, Physical, and Engineering Sciences*, *369*(1943), 2058–2072. doi:10.1098/rsta.2010.0341

Ferry, J. G., & Lessner, D. J. (2008). Methanogenesis in marine sediments. *Annals of the New York Academy of Sciences*, *1125*, 147–157. http://doi.org/10.1196/annals.1419.007

Gamo, T., Tsunogai, U., Ichibayashi, S., Chiba, H., Obata, H., Oomori, T., … Sano, Y. (2010). Microbial carbon isotope fractionation to produce extraordinarily heavy methane in

aging hydrothermal plumes over the southwestern Okinawa Trough. *Geochemical Journal*, *44*(6), 477–487.

Grant, N. J., & Whiticar, M. J. (2002). Stable carbon isotopic evidence for methane oxidation in plumes above Hydrate Ridge, Cascadia Oregon Margin. *Global Biogeochemical Cycles*, *16*(4), 13–71. doi:10.1029/2001GB001851

Grossart, H.-P., Frindte, K., Dziallas, C., Eckert, W., & Tang, K. W. (2011). Microbial methane production in oxygenated water column of an oligotrophic lake. *Proceedings of the National Academy of Sciences*, *108*(49), 19657–19661. http://doi.org/10.1073/pnas.1110716108

Jakobs, G., Rehder, G., Jost, G., Kie??lich, K., Labrenz, M., & Schmale, O. (2013). Comparative studies of pelagic microbial methane oxidation within the redox zones of the Gotland Deep and Landsort Deep (central Baltic Sea). *Biogeosciences*, *10*(12), 7863–7875. doi:10.5194/bg-10-7863-2013

Jørgensen, B. B., & Kasten, S. (2006). Sulfur Cycling and Methane Oxidation. *Marine Geochemistry*, 271–309. http://doi.org/10.1007/3-540-32144-6_8

Kinnaman, F. S., Valentine, D. L., & Tyler, S. C. (2007). Carbon and hydrogen isotope fractionation associated with the aerobic microbial oxidation of methane, ethane, propane and butane. *Geochimica et Cosmochimica Acta*, *71*(2), 271–283. doi:10.1016/j.gca.2006.09.007

Mann, M. E., Bradley, R. S., & Hughes, M. K. (1999). Northern hemisphere temperatures during the past millennium: Inferences, uncertainties, and limitations. *Geophysical Research Letters*, *26*(6), 759–762. http://doi.org/10.1029/1999GL900070

McGinnis, D. F., Greinert, J., Artemov, Y., Beaubien, S. E., & W??est, A. (2006). Fate of rising methane bubbles in stratified waters: How much methane reaches the atmosphere? *Journal of Geophysical Research: Oceans*, *111*(9), 1–15. http://doi.org/10.1029/2005JC003183

Myhre, G., D. Shindell, F.-M. Bréon, W. Collins, J. Fuglestvedt, J. Huang, D. Koch, J.-F. Lamarque, D. Lee, B. Mendoza, T. Nakajima, A. Robock, G. Stephens, T. Takemura and H. Zhang, 2013: Anthropogenic and Natural Radiative Forcing. In: *Climate Change 2013: The Physical Science Basis*. Contribution of Working Group I to the Fifth Assessment Report of the Intergovernmental Panel on Climate Change [Stocker, T.F., D. Qin, G.-K. Plattner, M. Tignor, S.K. Allen, J. Boschung, A. Nauels, Y. Xia, V. Bex and P.M. Midgley (eds.)]. Cambridge University Press, Cambridge, United Kingdom and New York, NY, USA.

Omelchenko, M. V., Vasilyeva, L. V., & Zavarzin, G. A. (1993). Psychrophilic methanotroph from tundra soil. *Current Microbiology*, *27*(5), 255–259. http://doi.org/10.1007/BF01575988

Reeburgh, W. (2007). Oceanic methane biogeochemistry. *American Chemical Society*, *107*, 486–513. doi:10.1021/cr050362v

Rice, a L., Gotoh, a a, Ajie, H. O., & Tyler, S. C. (2001). High-Precision Continuous-Flow Measurement of δ 13C and δD of Atmospheric CH4. *Analytical Chemistry*, *73*(17), 4104–4110. http://doi.org/10.1021/ac0155106

Roberts, H. M., & Shiller, A. M. (2015). Determination of dissolved methane in natural waters using headspace analysis with cavity ring-down spectroscopy. *Analytica Chimica Acta*, *856*, 68–73. doi:10.1016/j.aca.2014.10.058

Ruppel, C. D. (2011) Methane Hydrates and Contemporary Climate Change. *Nature Education Knowledge* 3(10):29

Schubert, C. J., Coolen, M. J. L., Neretin, L. N., Schippers, A., Abbas, B., Durisch-Kaiser, E., … Kuypers, M. M. M. (2006). Aerobic and anaerobic methanotrophs in the Black Sea water column. *Environmental Microbiology*, *8*(10), 1844–1856. http://doi.org/10.1111/j.1462-2920.2006.01079.x

Scott, K. M., Lu, X., Cavanaugh, C. M., & Liu, J. S. (2004). Optimal methods for estimating kinetic isotope effects from different forms of the Rayleigh distillation equation. *Geochimica et Cosmochimica Acta*, *68*(3), 433–442. doi:10.1016/S0016-7037(03)00459-9

Seifert, R., Nauhaus, K., Blumenberg, M., Kr??ger, M., & Michaelis, W. (2006). Methane dynamics in a microbial community of the Black Sea traced by stable carbon isotopes in vitro. *Organic Geochemistry*, *37*(10), 1411–1419. http://doi.org/10.1016/j.orggeochem.2006.03.007

Shakhova, N., Semiletov, I., & Panteleev, G. (2005). The distribution of methane on the Siberian Arctic shelves : Implications for the marine methane cycle, *32*, 4–7. http://doi.org/10.1029/2005GL022751

Shakhova, N. E., Alekseev, V. A., & Semiletov, I. P. (2010a). Predicted methane emission on the East Siberian shelf. *Doklady Earth Sciences*, *430*(2), 190–193. http://doi.org/10.1134/S1028334X10020091

Shakhova, N., Semiletov, I., Leifer, I., Salyuk, A., Rekant, P., & Kosmach, D. (2010b). Geochemical and geophysical evidence of methane release over the East Siberian Arctic Shelf. *Journal of Geophysical Research: Oceans*, *115*(8), 1–14. http://doi.org/10.1029/2009JC005602

Shakhova, N., Semiletov, I., Sergienko, V., Lobkovsky, L., Yusupov, V., Salyuk, A., … Gustafsson, O. (2015). The East Siberian Arctic Shelf: towards further assessment of permafrost-related methane fluxes and role of sea ice. *Philosophical Transactions. Series A, Mathematical, Physical, and Engineering Sciences*, *373*(2052), 20140451–. http://doi.org/10.1098/rsta.2014.0451

Tang, K. W. . B., McGinnis, D. F. . D., Frindte, K. ., Brüchert, V. ., & Grossart, H.-P. . F. (2014). Paradox reconsidered: Methane oversaturation in well-oxygenated lake waters.

Limnology and Oceanography, *59*(1), 275–284. http://doi.org/10.4319/lo.2014.59.1.0275

Templeton, A. S., Chu, K. H., Alvarez-Cohen, L., & Conrad, M. E. (2006). Variable carbon isotope fractionation expressed by aerobic CH4-oxidizing bacteria. *Geochimica et Cosmochimica Acta*, *70*(7), 1739–1752. http://doi.org/10.1016/j.gca.2005.12.002

Trotsenko, Y. A., & Khmelenina, V. N. (2005). Aerobic methanotrophic bacteria of cold ecosystems. *FEMS Microbiology Ecology*, *53*(1), 15–26. http://doi.org/10.1016/j.femsec.2005.02.010

Wagner, D., Gattinger, A., Embacher, A., Pfeiffer, E. M., Schloter, M., & Lipski, A. (2007). Methanogenic activity and biomass in Holocene permafrost deposits of the Lena Delta, Siberian Arctic and its implication for the global methane budget. *Global Change Biology*, *13*(5), 1089–1099. http://doi.org/10.1111/j.1365-2486.2007.01331.x

Whiticar, M. J. (1999). Carbon and hydrogen isotope systematics of bacterial formation and oxidation of methane. *Chemical Geology*, *161*(1-3), 291–314. doi:10.1016/s0009-2541(99)00092-3

Whiticar, M. J., Faber, E., & Schoell, M. (1986). Biogenic methane formation in marine and freshwater environments: CO2 reduction vs. acetate fermentation-Isotope evidence. *Geochimica et Cosmochimica Acta*, *50*(5), 693–709. doi:10.1016/0016-7037(86)90346-7

Whiticar, M.J., Faber, E., 1986. Methane oxidation in sediment and water column environments — isotope evidence. Org. Geochem. 10, 759–768.

Wiesenburg, D. A., & Guinasso Jr, N. L. (1979). Equilibrium solubilities of methane, carbon monoxide, and hydrogen in water and sea water. *Journal of Chemical and Engineering Data*, *24*(4), 356–360. doi:10.1021/je60083a006

Wolin, M. J., & Miller, T. L. (1987). Bioconversion of organic carbon to CH4 and CO2. *Geomicrobiol J*, *5*(April), 239–260. doi:10.1080/01490458709385972

9 Appendix

9.1 Starting conditions – Brunnsviken

Starting conditions Brunnsviken				
Depth (m)	Concentration (nM)	Standard deviation (nM)	δ13C-CH4 (‰)	Standard deviation (‰)
0	1154	72.48	-50.81	3.22
2	1007	6.87	-47.26	0.23
4	907	46.68	-44.07	0.64
5	889	16.23	-46.56	0.25
7	874	6.24	-43.49	0.09
8	1177	7.68	-51.42	0.27
9	56318	609.37	-70.60	1.84

Table 9.1 – Start concentration and carbon isotope composition from the pilot experiment in Brunnsviken.

9.1.1 Time series – Brunnsviken

2m Time series				
Days	Concentration (nM)	Standard deviation (nM)	δ13C-CH4 (‰)	Standard deviation (‰)
0	1007	6.87	-47.26	0.23
7	123	20.80	7.46	1.98
14	149	13.65	7.78	1.61
21	136	16.31	8.62	3.29

Table 9.2 – Time series for 2m depth in Brunnsviken.

5m Time series				
Days	Concentration (nM)	Standard deviation (nM)	δ13C-CH4 (‰)	Standard deviation (‰)
0	889	16.23	-46.56	0.25
7	79	27.35	22.49	8.82
14	67	8.78	27.65	2.18
21	118	32.22	11.88	9.66

Table 9.3 Time series of 5m depth in Brunnsviken

9m Time series				
Days	Concentration (nM)	Standard deviation (nM)	δ13C-CH4 (‰)	Standard deviation (‰)
0	56318	609.37	-70.60	1.84
7	704	537.12	-47.50	20.66
14	35811	2199.89	-71.91	0.70
21	18904	21067.98	-52.60	12.67

Table 9.4 – 9m time series conducted in Brunnsviken

9.2 East Siberian Shelf – Time series

Water concentration 1 incubated in 20°C				
Days	Concentration (nM)	Standard deviation (nM)	δ13C-CH4 (‰)	Standard deviation (‰)
0	60	1.22	-45.05	0.19
2	68		-44.09	
14	110	7.61	-43.69	1.66
28	61		-44.78	
70	56		-45.27	
115	137		-44.46	

Table 9.5 – Time series of experiment 1 on the East Siberian Shelf where only spiked water was incubated in 20°C.

Water concentration 2				
Days	Concentration (nM)	Standard deviation (nM)	δ13C-CH4 (‰)	Standard deviation (‰)
0	665	6.45	-45.44	0.14
2	551		-45.30	
14	580	22.73	-45.23	0.43
28	639		-45.97	
45	623		-45.60	
70	530		-45.91	
115	569		-45.38	

Table 9.6 – Experiment 2 time series where water was incubated in 20°C.

Water incubated in 4°C				
Days	Concentration (nM)	Standard deviation (nM)	δ13C-CH4 (‰)	Standard deviation (‰)
0	509	44.55	-45.81	0.08
19	498	39.47	-45.58	0.09
42	448	31.22	-46.11	0.49

Table 9.7 Time series of experiment 3 where water was incubated in 4°C.

Water and sediment incubated in 20°C				
Days	Concentration (nM)	Standard deviation (nM)	δ13C-CH4 (‰)	Standard deviation (‰)
0	438	31.10	-45.26	0.13
9	437		-45.34	
20	382		-45.56	
33	441		-45.99	
36	501		-45.24	
54	460		-45.84	
77	361		-45.24	

Table 9.8 – Experiment 4 time series where water and sediment was incubated in 20°C.

Water and sediment incubated in 4°C				
Days	Concentration (nM)	Standard deviation (nM)	δ13C-CH4 (‰)	Standard deviation (‰)
0	427	27.35	-45.26	0.16
9	445		-44.13	
20	326		-40.74	
33	82		-19.23	
36	95		-22.07	
54	2			
77	8			
79	8	0.26		
79	7			

Table 9.9 – Time series of experiment 5 where water and sediment was incubated in 4°C.